# Multiparticle and higher-spin tests of quantum mechanics using parametric down-conversion

W. J. Munro
*Physics Department, University of Waikato, Hamilton, New Zealand*

M. D. Reid
*Physics Department, The University of Queensland, Brisbane, Australia*
(Received 14 February 1994)

We show that various experimental configurations using correlated photon-number states are predicted to violate many forms of Bell's inequality. This test is potentially one of macroscopic quantum mechanics in that violations are predicted for situations where large numbers of photons are detected at a single detector at a time. The configurations also allow higher-spin tests of quantum mechanics. We indicate how the violations of Bell inequalities might be achieved with both parametric amplification and parametric oscillation. The effect of photodetection inefficiencies is analyzed. In order to investigate the potential for Bell-inequality tests in the high-intensity regime of recent experiments where detection efficiencies may be very high, we introduce a simple model for the effect of electronic noise that introduces a poor resolution of the photon number detected.

PACS number(s): 03.65.Bz

## I. INTRODUCTION

Bell's theorem [1,2] provides a way of testing the predictions of quantum mechanics against those of classical (local realistic) theories [3]. For certain experiments quantum mechanics allows a violation of Bell inequalities predicted from the assumptions of local realism. To date experiments have shown a violation of the classical Bell inequalities in support of quantum mechanics [4]. A number of the recent experiments use parametric down-conversion to generate a correlated photon pair [5] which exhibits this extreme quantum behavior [6–9]. In these experiments, the photons of each pair are individually incident on one of two spatially separated "analyzers" (polarizers or beam splitters or an alternative measuring apparatus). There are thus (assuming each particle is detected) two possible outcomes at each analyzer, in analogy with the original spin-$\frac{1}{2}$ formulation of the Bell inequality tests.

In this paper we focus attention on the use of correlated photon-number states produced through parametric down-conversion to test quantum mechanics in situations where more than one photon is simultaneously incident on each analyzer [10–12]. There is thus an equivalence to a higher-spin test of quantum mechanics. Our calculations are models for extensions of the experiments of Shih and Alley [6], Ou and Mandel [7], and Rarity and Tapster [8]. Various Bell inequality tests of quantum theory for higher-spin states have been formulated previously [13–15], but have not been realized experimentally to date. In this paper we consider previous and alternative formulations as applied to correlated number states, comparing the quantum prediction for the degree of departure from classical predictions in each case. In the first instance we use a simple model interaction Hamiltonian to describe the basic quantum nature of the correlated photon states generated by down-conversion. The effect of detection inefficiencies is included. We then present a more complete calculation of the field generated using an optical parametric oscillator, where the down-conversion takes place inside an optical cavity. We consider this situation in some detail since the use of a cavity configuration may enable enhancement of the conversion efficiency for signal and idler photons of a particular mode. Finally we consider the situation where we can have high photodetection efficiencies, but a poorer resolution of the photon number due to electronic noise. This result is part of a preliminary investigation applicable to the recent experiment of Smithey *et al.* [16], where quantum photon-number correlations are measured between two macroscopic pulses produced by parametric down-conversion. Here the use of photodiodes implies a high detection efficiency. This regime is of particular interest since a strong test of Bell's inequality not limited by auxiliary assumptions [17] might be possible. However, the new limitation provided by electronic noise which will limit the resolution of photon number detected must be considered.

We point out that the multiparticle tests described here are different from those proposed recently by Greenberger *et al.* [18,19]. In their case the particles are spatially separated so that there is still only one particle incident on each analyzer. An extension of the Greenberger-Horne-Zeilinger result as applied to situations of more than one photon per analyzer has been considered by us [20].

## II. CLASSICAL BELL INEQUALITIES APPLYING TO THE EXPERIMENTAL CONFIGURATIONS

Figures 1 and 2 depict schematically experimental configurations which might be used to test for violations of

 

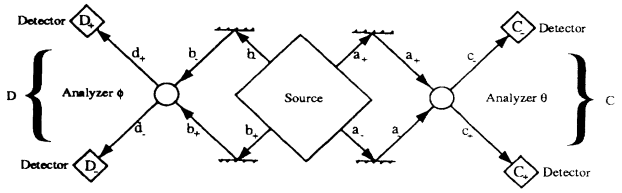


FIG. 1. Schematic diagram of the transformations involved in the experimental arrangement to test Bell's inequalities using polarizers–beam splitters.

Bell inequalities. In each case there are four input fields, which we will denote simply by $a_+, a_-$ and $b_+, b_-$, as indicated in Figs. 1 and 2. Figure 1 is the arrangement which most closely resembles that considered by Clauser and Shimony [2] and Aspect *et al.* [4]. The inputs undergo the following transformations, which are realized by polarizers, although they could also be obtained by beam splitters if $a_+, a_-$ are spatially separated inputs. This second interferometric arrangement was considered by Reid and Walls [21]:

$$\begin{aligned} c_+ &= a_+ \cos\theta + a_- \sin\theta, \\ c_- &= -a_+ \sin\theta + a_- \cos\theta, \\ d_+ &= b_+ \cos\phi + b_- \sin\phi, \\ d_- &= -b_+ \sin\phi + b_- \cos\phi. \end{aligned} \tag{2.1}$$

We also consider the alternative configuration (Fig. 2) where phase shifts and beam splitters generate the mixing of the input beams:

$$\begin{aligned} c_+ &= \frac{a_+ + i\exp[i\theta]\, a_-}{\sqrt{2}}, \\ c_- &= \frac{ia_+ + \exp[i\theta]\, a_-}{\sqrt{2}}, \\ d_+ &= \frac{b_+ + i\exp[i\phi]\, b_-}{\sqrt{2}}, \\ d_- &= \frac{ib_+ + \exp[i\phi]\, b_-}{\sqrt{2}}. \end{aligned} \tag{2.2}$$

The experiments of Rarity and Tapster [8] obtained violations of Bell's inequalities using such phase shifts. Transformations of this type were suggested by Horne *et al.* [22] and also considered by Reid and Walls [21]. The transformation brought about by the analyzer apparatus at each of the spatially separated locations $C$ and $D$ is followed by detection. One thus performs a measurement at each of the spatially separated locations, $\theta$ and $\phi$ indicating the choices made by the experimenter.

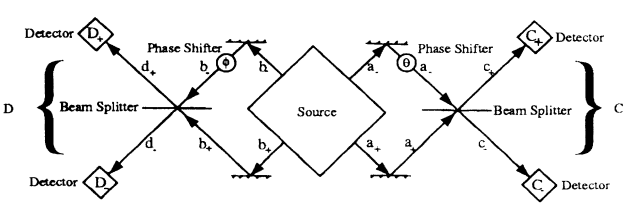


FIG. 2. Schematic diagram of the transformations involved in the experimental arrangement to test Bell's inequalities using phase shifters and beam splitters.

It is necessary to summarize the classical prediction for the results of the possible experiments depicted in Figs. 1 and 2. This is done by presenting various forms of Bell's inequalities adapted for the configurations. Of interest to us is the situation where $N$ quanta are incident on the analyzers at both $C$ and $D$. We denote the number of quanta detected at $C_+$ by $n_1$ and the number of quanta detected at $D_+$ by $n_2$. In fact the result is dependent on the angle choices $\theta$ and $\phi$ and we will sometimes write $n_1(\theta)$ and $n_2(\phi)$ to indicate this. The possible values of $n_1$ and $n_2$ range in integer steps from 0 to $N$. In the absence of loss, one has $N - n_1$ and $N - n_2$ photons at $C_-$ and $D_-$, respectively. The measured quantities are the photon numbers $c_+^\dagger c_+$ and $d_+^\dagger d_+$. Introducing the notation

$$\begin{aligned} J_z^{(1)}(\theta) &= \frac{c_+^\dagger c_+ - c_-^\dagger c_-}{2}, \\ J_x^{(1)}(\theta) &= \frac{c_+^\dagger c_- + c_-^\dagger c_+}{2}, \\ J_y^{(1)}(\theta) &= \frac{c_+^\dagger c_- - c_-^\dagger c_+}{2i}, \\ J_z^{(1)} &= \frac{a_+^\dagger a_+ - a_-^\dagger a_-}{2}, \\ J_x^{(1)} &= \frac{a_+^\dagger a_- + a_-^\dagger a_+}{2}, \\ J_y^{(1)} &= \frac{a_+^\dagger a_- - a_-^\dagger a_+}{2i}, \end{aligned} \tag{2.3}$$

one establishes the well-known Schwinger relation between the boson description and angular momentum operators $J_x, J_y, J_z$. The transformation of the $a_+, a_-$ into the $c_+, c_-$ given by (2.1) is equivalent to a rotation of the angular momentum operators $(J_x, J_y, J_z)$. The boson system with $N$ quanta incident at $C$ and $D$ is equivalent to the $\frac{N}{2}$-spin system. We define $J_z^{(2)}(\phi)$, $J_x^{(2)}(\phi)$, $J_y^{(2)}(\phi)$, $J_z^{(2)}$, $J_x^{(2)}$, and $J_y^{(2)}$ to be the spin operators defined similarly in terms of the operators $d_+$ and $d_-$ and $b_+$ and $b_-$ , so that, for example, $J_z^{(2)}(\phi) = \frac{d_+^\dagger d_+ - d_-^\dagger d_-}{2}$. The result of a measurement of $J_z^{(1)}(\theta)$ and $J_z^{(2)}(\phi)$ at $C_+$ and $D_+$ is given respectively by $m_1 = (2n_1 - N)/2$ and $m_2 = (2n_2 - N)/2$. Again, we will sometimes write $m_1$ as $m_1(\theta)$ and $m_2$ as $m_2(\phi)$ to indicate the dependence of the measurement on the analyzer angles.

One can determine experimentally the joint probability $P(m_1, m_2)$ for the results $m_1$ and $m_2$. Mermin [13] has predicted the following Bell inequality for experiments where the set of possible outcomes for $m_1$ and $m_2$ are integers between $-N/2$ and $N/2$. The inequality he derived from the classical premises of locality and realism is

$$\begin{aligned} \Delta_N = \langle m_1(\theta) m_2(\phi') \rangle + \langle m_1(\phi) m_2(\phi') \rangle \\ - \frac{N}{2} \langle |m_1(\theta) - m_2(\phi)| \rangle \leq 0. \end{aligned} \tag{2.4}$$

More recently Braunstein and Caves [14] have developed a classical information-theoretic Bell inequality. Following Braunstein and Caves, one defines the information content of the measurements of $J_z^{(1)}(\theta)$ and $J_z^{(2)}(\phi)$ as $I(m_1,m_2) = -\ln P(m_1,m_2)$. The information obtained upon measurement of $J_z^{(2)}(\phi)$ at D is

$$I(m_2) = -\ln P(m_2),$$

$P(m_i)$ being the probability of obtaining the result $m_i$. The information obtained when one measures the value $m_1$, given that one has already measured $m_2$, is defined as

$$I(m_1/m_2) = -\ln P(m_1/m_2).$$

The average value for this conditional information is

$$H\left[J_z^{(1)}(\theta)/J_z^{(2)}(\phi)\right] = \sum_{m_1,m_2} P(m_1,m_2) I(m_1/m_2). \quad (2.5)$$

One abbreviates the notation as follows: $H\left[J_z^{(1)}(\theta)/J_z^{(2)}(\phi)\right] = H(\theta,\phi)$. The Bell inequality derived by Braunstein and Caves [14] is

$$H(\theta/\phi) \leq H(\theta/\phi') + H(\phi'/\theta') + H(\theta'/\phi). \quad (2.6)$$

The approach taken by Drummond [10] is to consider the joint probability $P(m_1 = N/2, m_2 = N/2)$. This approach is particularly useful for optical experiments of the type considered by Clauser *et al.* [2,17], where the polarizers are single channeled and it is thus not possible to detect photons at the locations $C_-$ and $D_-$. The Bell inequality considered by Drummond is a modification of that derived by Clauser and Horne and Clauser, Horne, Shimony, and Holt (CHSH) [2,17]. Let us denote $P(N/2,N/2)$ as $P_N(\theta,\phi)$ to indicate specifically the angular dependence of the measurements. We define more generally $P_n(\theta,\phi)$ as the joint probability of detecting $n$ photons at $C_+$ and $n$ photons at $D_+$ to allow for situations where not all of the $N$ photons incident on each analyzer are detected. The generalization of the Bell–Clauser-Horne-Shimony-Holt inequality is (we outline the derivation of this in Sec. VI of the paper)

$$B_n = \frac{P_n(\theta,\phi) - P_n(\theta,\phi') + P_n(\theta',\phi) + P_n(\theta',\phi')}{P_n(\theta',-) + P_n(-,\phi)} \leq 1. \quad (2.7)$$

Here $P_n(\theta',-)$ and $P_n(-,\phi)$ are the marginal probabilities for detecting $n$ photons at $C_+$ and $n$ photons at $D_+$, respectively. A violation of this inequality corresponds to $B_n > 1$.

One may also consider "product" inequalities. In many situations $P_N(\theta,\phi)$ is small and hence an experimenter must perform many runs before obtaining sufficient data. It may be advantageous to hence examine the product inequalities defined below where all the data contribute. We assign a value to the variable $E_i^\theta$ of $+1$ or $-1$ if the $i$th quantum incident at $C$ is at $C_+$ or $C_-$, respectively. The variable $E_i^\phi$ is defined similarly at the location $D$. If $N$ quanta are incident at each location $C$ and $D$, one defines the product

$$E_N^1(\theta) E_N^2(\phi), \quad (2.8)$$

where $E_N^1(\theta) = \prod_{i=1}^N E_i^\theta$ and $E_N^2(\phi) = \prod_{j=1}^N E_j^\phi$. We now define $E_N(\theta,\phi)$ to be the expected value of this product. Thus

$$E_N(\theta,\phi) = \sum_{i,j=0}^{N} P_{i,N-i,j,N-j}(\theta,\phi)\,(-1)^{2N-i-j}\,(1)^{i+j}, \quad (2.9)$$

where $P_{i,N-i,j,N-j}(\theta,\phi)$ is the probability of detecting $i$, $N-i$, $j$, and $N-j$ photons at $C_+$, $C_-$, $D_+$, and $D_-$, respectively. For situations where the $i$th quantum is not detected (due to poor efficiency of detectors for example), one may assign $E_i^\theta = 0$ and generalize the expression (2.9) accordingly. One may consider more general situations where we select to measure an $E_n(\theta,\phi)$, selecting a total of $n$ photons at both $C$ and $D$, where $n$ is not necessarily equal to $N$, the number of photons incident on the analyzers. The result for $|E_i^\theta|$ is always bounded by 1, and a direct application of Bell's 1971 proof leads [1] to the following inequality (the derivation is outlined in Sec. VI of this paper):

$$S_n = |E_n(\theta,\phi) - E_n(\theta,\phi') + E_n(\theta',\phi) + E_n(\theta',\phi')| \leq 2. \quad (2.10)$$

In order to account for real experiments performed where photon detection efficiencies are very poor and not all of $N$ quanta incident on each analyzer will be detected, Clauser and Horne and CHSH derived modified inequalities for the $N = 1$ case, based on additional auxiliary assumptions [1,2,17]. The inequalities derived in our case are identical in form to the inequalities (2.7) and (2.10) presented above, except that the probabilities and expectation values are calculated over the subensemble where $n$ quanta are detected at *both* $C$ and $D$. The implication of the Clauser-Horne analysis for the inequality (2.7) is that the marginal probabilities are replaced by joint probabilities. The $P_n(\theta,-)$ now becomes the joint probability for detecting $n$ quanta at $C_+$ *and* $n$ quanta at $D$, with the analyzer at $D$ removed. We will thus also refer to Eq. (2.7) as the Clauser-Horne inequality. The implication for the product inequality (2.10) is the replacement of $E_n(\theta,\phi)$ with the normalized $E_n(\theta,\phi)$ (see Sec. VI) defined as

$$E_n(\theta,\phi) = \frac{\sum_{i,j=0}^{n} P_{i,n-i,j,n-j}(\theta,\phi)\,(-1)^{2n-i-j}\,(1)^{i+j}}{\sum_{i,j=0}^{n} P_{i,n-i,j,n-j}(\theta,\phi)}. \quad (2.11)$$

These modified inequalities are weaker since one requires, for their derivation, the additional auxiliary or supplementary assumptions. These are discussed in Sec. VI.

## III. QUANTUM PREDICTIONS FOR CORRELATED PHOTON-NUMBER STATES

We first present calculations based on the input state [10]

$$|\varphi\rangle = \frac{\left[a_+^\dagger b_+^\dagger + a_-^\dagger b_-^\dagger\right]^N |0\rangle}{N!\sqrt{N+1}} = \frac{1}{\sqrt{N+1}} \sum_{r=0}^{N} |r\rangle_{a_+} |r\rangle_{b_+} |N-r\rangle_{a_-} |N-r\rangle_{b_-}, \quad (3.1)$$

where, for example $|r\rangle_{b_+}$, is the $r$-photon number state for $b_+$. Here we have a total of $N$ quanta at $C$ and $N$ quanta at $D$. For $N = 1$, this correlated superposition state (or "entangled state") is analogous to that generated in the experiments of Aspect *et al.* [4]. In these experiments $a_+$ and $a_-$ represent orthogonal polarizations.

The input state (3.1) can be expanded in terms of the eigenstates $|m_1, m_2\rangle$ of $J_z^{(1)}(\theta)$ and $J_z^{(2)}(\theta)$,

$$|\varphi\rangle = \frac{1}{\sqrt{N+1}} \sum_{r=0}^{N} \left| \frac{N}{2} - r, \frac{N}{2} - r \right\rangle_\theta, \quad (3.2)$$

where $J_z^{(2)}(\theta) J_z^{(1)}(\theta) |m_1, m_2\rangle = m_1 m_2 |m_1, m_2\rangle$. The expansion holds regardless of the choice of $\theta$. This state is identical in form to the zero total-spin state considered by Mermin [13] and Caves and Braunstein [14], except that $m_2$ has changed sign. One can calculate the joint probabilities $P(m_1(\theta), m_2(\phi))$ and expectation values $\langle m_1(\theta) m_2(\phi)\rangle$ and establish a violation of the classical inequalities (2.4), (2.6), (2.7), and (2.10), based on the apparatus of Fig. 1. Since rotation of both sets $(a_+, a_-)$ and $(b_+, b_-)$ by an angle $\theta$ in accordance with the transformation (2.1) leaves the state (3.1) invariant, we can select our axes to coincide with the first angle $\theta$ associated with the measurement at $C$. The transformation we consider is then

$$\begin{aligned} c_+ &= a_+, \\ c_- &= a_-, \\ d_+ &= b_+ \cos\varphi + b_- \sin\varphi, \\ d_- &= -b_+ \sin\varphi + b_- \cos\varphi, \end{aligned} \quad (3.3)$$

where $\varphi = \phi - \theta$. Calculation of $P(m_1(\theta), m_2(\phi))$ thus proceeds by evaluating $P(m_1(0), m_2(\varphi))$ upon us noting that $|\varphi\rangle$ can be expressed in terms of the measured modes as

$$|\varphi\rangle = \frac{\left[c_+^\dagger d_+^\dagger \cos\varphi - c_+^\dagger d_-^\dagger \sin\varphi + c_-^\dagger d_+^\dagger \sin\varphi + c_-^\dagger d_-^\dagger \cos\varphi\right]^N |0\rangle}{N!\sqrt{N+1}} = \sum_{n_1, n_2 = 0}^{N} C_{n_1 n_2} |n_1\rangle_{c_+} |N-n_1\rangle_{c_-} |n_2\rangle_{d_+} |N-n_2\rangle_{d_-}. \quad (3.4)$$

Now $P(m_1, m_2)$ is the probability of detecting $n_1$ and $n_2$ photons at $C_+$ and $D_+$, respectively, where $n_i = m_i + N/2$. Thus evaluating the relevant coefficients $C_{n_1 n_2}$ we obtain

$$P(m_1(\theta), m_2(\phi)) = \frac{n_1! n_2! (N-n_1)! (N-n_2)!}{N+1} \left[ \sum_{r=0}^{\min(n_1, n_2)} \frac{(-1)^{n_1 - r} \cos^{N-n_1-n_2+2r}\varphi \sin^{n_1+n_2-2r}\varphi}{r!(n_1-r)!(n_2-r)!(N-n_1-n_2-r)!} \right], \quad (3.5)$$

where $n_1 = m_1(\theta) + N/2$ and $n_2 = m_2(\phi) + N/2$. It is noted that since the joint probabilities are

$$P(m_1, m_2) = \frac{|C_{n_1 n_2}|^2}{\sum_{n_1, n_2 = 0}^{N} |C_{n_1 n_2}|^2}, \quad (3.6)$$

we can write $P(m_1, m_2)$ in terms of correlation functions (as also follows from the standard photon-count formula)

$$P(m_1, m_2) = \frac{\binom{N}{n_1}\binom{N}{n_2} \left\langle : \left(c_+^\dagger c_+\right)^{n_1} \left(c_-^\dagger c_-\right)^{N-n_1} \left(d_+^\dagger d_+\right)^{n_2} \left(d_-^\dagger d_-\right)^{N-n_2} : \right\rangle}{\left\langle : \left(c_+^\dagger c_+ + c_-^\dagger c_-\right)^N \left(d_+^\dagger d_+ + d_-^\dagger d_-\right)^N : \right\rangle}. \quad (3.7)$$

Thus

$$P_N(\theta,\phi)=\frac{\left\langle :c_+^{\dagger N}c_+^N d_+^{\dagger N}d_+^N:\right\rangle}{\left\langle :\left(c_+^\dagger c_+ + c_-^\dagger c_-\right)^N\left(d_+^\dagger d_+ + d_-^\dagger d_-\right)^N:\right\rangle} \tag{3.8}$$

and

$$P_N(\theta,-)=\frac{\left\langle :c_+^{\dagger N}c_+^N\left(d_+^\dagger d_+ + d_-^\dagger d_-\right)^N:\right\rangle}{\left\langle :\left(c_+^\dagger c_+ + c_-^\dagger c_-\right)^N\left(d_+^\dagger d_+ + d_-^\dagger d_-\right)^N:\right\rangle}. \tag{3.9}$$

The product $E_N(\theta,\phi)$ is written

$$E_N(\theta,\phi)=\frac{\left\langle :\left(c_+^\dagger c_+ - c_-^\dagger c_-\right)^N\left(d_+^\dagger d_+ - d_-^\dagger d_-\right)^N:\right\rangle}{\left\langle :\left(c_+^\dagger c_+ + c_-^\dagger c_-\right)^N\left(d_+^\dagger d_+ + d_-^\dagger d_-\right)^N:\right\rangle}. \tag{3.10}$$

Figures 3–5 depict the violation of the classical inequalities for varying values of $N$. The violations predicted in Figs. 3 and 4 have been calculated previously by Mermin [13] and Drummond [10] and are presented here for the sake of comparison. We have also calculated the violations possible using the phase-shift–beam-splitter appartus of Fig. 2. Because the violation is present for $N$ particles incident on each analyzer even for $N$ large, the proposed experiment is potentially one of quantum mechanics at a macroscopic level [10]. We note that the Clauser-Horne experiment where $P_N(\theta,\phi)$ is measured has a potential disadvantage for larger $N$, since with $N$ photons incident the actual probability $P_N(\theta,\phi)$ can be small, making the experiment difficult. The product inequalities have the advantage that all outcomes contribute to the data collected for the experiment.

It is important to discuss precisely in what sense our test of quantum mechanics discussed here is macroscopic. We point out that, since at each detector one might detect the whole range of $N, N-1,\ldots,0$ photons, the final state produced at the detectors is not a simple superposition of macroscopically distinct states (a "Schrödinger-cat" state [23]). Rather we have a macroscopic (with $N$ large) number of states which are microscopically distinct superposed, so that only some pairs are macroscopically separated. In the tests proposed here the distinction is being made between states which are microscopically distinct in order to gain violations of Bell inequalities, in that we gain the contradiction with classical theories by detecting all $N$ photons. For example, in the Clauser-Horne measurement needed for inequality (2.7), information is gained about all of the $N$ photons in that they are all detected in the + position. The effect of detecting only $N-1$ photons, so that the location of one photon is not specified, is to decrease or lose the contradiction with classical theories. This effect was pointed out by Drummond [10] with respect to the case shown in Fig. 4. We illustrate this effect in Figs. 4 and 5 by calculating $B_N$ and $E_N$ with $n=N-1$ so that a total of $N-1$ photons are detected, the $N$th photon being lost. Quantum mechanics predicts the joint probability functions $P_n(\theta,\phi)$ and $P_n(\theta,-)$ (where $n$ is less than $N$ and no information is obtained about the remaining $N-n$ photons) to be given in this case by the moments $\langle :c_+^{\dagger n}c_+^n d_+^{\dagger n}d_+^n:\rangle/(n!)^2$ and $\langle :c_+^{\dagger n}c_+^n(d_+^\dagger d_+ + d_-^\dagger d_-)^n:\rangle/(n!)^2$, respectively, so that $B_n$ and $E_n(\theta,\phi)$ are readily calculated. This result follows directly from the standard photon-count formula. It is noted by comparing Figs. 4 and 5 that the sensitivity of the violation of the Bell inequalities to this loss of information about one photon is greater in the case of the product test. In the Clauser-Horne inequality considered by Drummond [10], a violation may be obtained for $n<N$ photons detected, provided a large number $N$ of photons is incident on the detectors. To conclude, the tests proposed here cannot be thought of as a test of macroscopic realism in the precise sense dis-

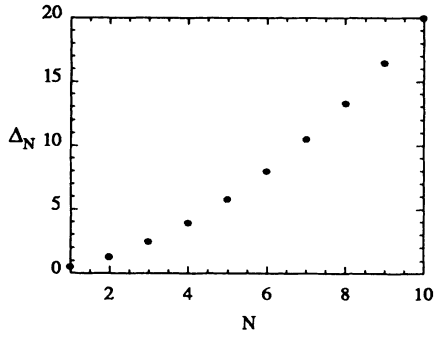


FIG. 3. Plot of the maximum violation ($\Delta_N$) of Mermin's higher-spin inequality for the state $\frac{\left(a_+^\dagger b_+^\dagger + a_-^\dagger b_-^\dagger\right)^N}{N!(N+1)^{1/2}}|0\rangle$. A violation of the inequality occurs for $\Delta_N>0$. The same results occur in both the polarizer and phase-shifter–beam-splitter arrangement (the angles are chosen for each $N$ to maximize the violation).

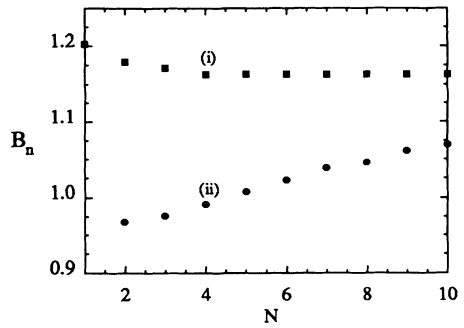


FIG. 4. Plot of the maximum value of $B_n$ (defined for the Clauser-Horne Bell inequality) versus $N$, the number of photon pairs in the correlated state $\frac{\left(a_+^\dagger b_+^\dagger + a_-^\dagger b_-^\dagger\right)^N}{N!(N+1)^{1/2}}|0\rangle$ for (i) $n=N$ and (ii) $n=N-1$, so that no information is obtained about one of the photons. A violation of the inequality occurs for $B_n>1$. The same results occur in the polarizer and phase-shifter–beam-splitter arrangements (the angles are chosen for each $N$ to maximize the violation).

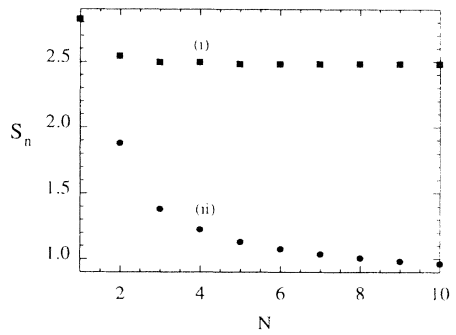


FIG. 5. Plot of the maximum value of $S_n$ (used in the product Bell inequality) versus $N$, the number of photon pairs in the correlated state $\frac{\left(a_+^\dagger b_+^\dagger + a_-^\dagger b_-^\dagger\right)^N}{N!(N+1)^{1/2}}|0\rangle$ for (i) $n = N$, (ii) $n = N-1$, so that no information is obtained about one of the photons. A violation of the inequality occurs for $S_n > 2$. The same results occur in the polarizer and phase-shifter–beam-splitter arrangement (the angles are chosen for each $N$ to maximize the violation).

cussed by Leggett [23], where one always distinguishes between two states macroscopically distinct. However, the interference generated by the multiple superposition states is sufficient to create a contradiction with quantum mechanics beyond the single-photon level.

One has to consider how to generate the state (3.1) or one similar to it, which will allow a test of quantum predictions against those of classical theories. In the following sections we suggest the use of parametric down-conversion. Experiments with $N = 1$ have already been performed using parametric down-conversion. The experiments of Rarity and Tapster [8] generate an entangled state of the type (3.1) with $N = 1$ using down-conversion directly. In the earlier experiments of Shih and Alley [6] and Ou and Mandel [7], the two signal and idler beams generated via down-conversion undergo transformations using beam splitters to generate a state similar to the four-mode state (3.1). The parametric interaction is used in these experiments to generate the correlated photon-number state $|1\rangle|1\rangle$ and hence to demonstrate violation of Bell's inequality in the microscopic regime [6–9]. Figures 6–8 depict schematically some experimental configurations which are used to test for violations of Bell inequalities in such a twin-beam experiment. The apparatus of Fig. 6 depicts the following transformations, which may be obtained with beam splitters and polarizers. Here $a_1$ and $b_1$ represent signal and idler beams, respectively,

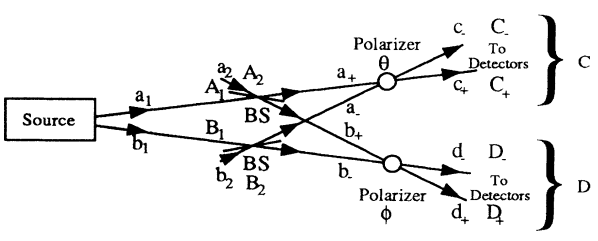


FIG. 6. Schematic diagram of the transformations involved in the experimental arrangement to test Bell's inequalities for the twin beam system using polarizers and beam splitters.

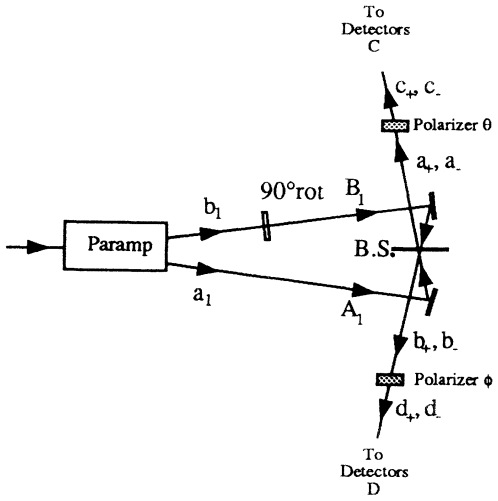


FIG. 7. Schematic diagram of the transformations used in the experiments of Shih and Alley [6] and Ou and Mandel [7]. Paramp denotes a parametric amplifier and BS the beam splitter.

$$a_+ = \frac{(a_1 + ia_2)}{\sqrt{2}}, \quad a_- = \frac{(b_2 + ib_1)}{\sqrt{2}},$$
$$b_+ = \frac{(ia_1 + a_2)}{\sqrt{2}}, \quad b_- = \frac{(ib_2 + b_1)}{\sqrt{2}}. \tag{3.11}$$

The $a_+, a_-$ and $b_+, b_-$ are then combined according to the transformation (2.1). This is essentially the scheme suggested by Reid and Walls [21], and Shih and Alley [6]. Alternative experimental arrangements have also been proposed [22,25]. We have shown previously [11] that the configuration of Fig. 6 can be used for multiparticle tests of Bell inequalities. The transformations (3.11) are identical to those produced in the experiment of Shih and Alley [6] and Ou and Mandel [7] (Fig. 7), where the two correlated photons generated via parametric down-conversion enter as inputs $a_1$ and $b_1$ of the beam splitter. In this arrangement the inputs $a_2$ and $b_2$ are orthogonal vacuum states. In the apparatus of Shih and Alley and Ou and Mandel the nonoverlapping modes $a_1$ and $b_1$ are thus incident as inputs of the same beam splitter and the emerging $a_\pm$ and $b_\pm$ are transformed using two spatially separated polarizers. It is also possible to transform the

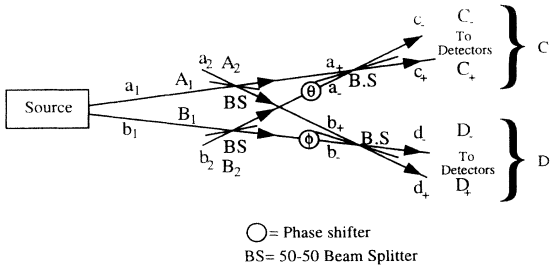


FIG. 8. Schematic diagram of the transformations involved in the experimental arrangement to test Bell's inequalities for the twin beam system using phase shifters and beam splitters.

$a_+, a_-$ and $b_+, b_-$ using phase shifts as described by the transformation (2.2). This arrangement is depicted in Fig. 8.

We now present calculations with the correlated photon number state $|N\rangle|N\rangle$ at the inputs $A_1$ and $B_1$ of Figs. 6–8. The inputs at $A_2$ and $B_2$ are vacuum states. It is possible to express [using the transformation (3.11)] the state generated in terms of the $a_+, a_-, b_+, b_-$ fields. One obtains [11]

$$\frac{1}{N!2^N}\sum_{r,r'=0}^{N}(-i)^{r+r'}\begin{bmatrix}N\\r\end{bmatrix}\begin{bmatrix}N\\r'\end{bmatrix}a_+^{\dagger\,N-r}b_+^{\dagger\,r}a_-^{\dagger\,r'}b_-^{\dagger\,N-r'}|0\rangle. \tag{3.12}$$

Here $|0\rangle$ represents the vacuum state for all modes. We see that one does not necessarily have $N$ quanta incident at both $C$ and $D$. Use is thus made of the weaker inequalities discussed, where the averages are defined only over the reduced subensemble where the selected number of quanta are actually detected at each of the outputs $C$ and $D$. The terms in the expansion (3.12) which are relevant for experiments where we select $N$ quanta detected at both $C$ and $D$ are

$$\frac{1}{N!2^N}\sum_{r=0}^{N}(-1)^r\begin{bmatrix}N\\r\end{bmatrix}^2 a_+^{\dagger\,N-r}b_+^{\dagger\,r}a_-^{\dagger\,r}b_-^{\dagger\,N-r}|0\rangle. \tag{3.13}$$

We see that for $N = 1$, this reduced state is identical in form to the four-mode state (3.1).

For $N > 1$, relating to the states of higher spin, differences exist. The results predicted for (3.13) will not be identical to those predicted by Mermin for the higher-spin state (3.2). The state (3.13) expressed in terms of the eigenstates $|m_1, m_2\rangle$ of $J_z^{(1)}$ and $J_z^{(2)}$ becomes

$$\frac{1}{2^N}\sum_{r=0}^{N}(-1)^r\begin{bmatrix}N\\r\end{bmatrix}\left|\frac{N}{2}-r,-\frac{N}{2}+r\right\rangle. \tag{3.14}$$

In this case the invariance under rotation to $J_z^{(1)}(\theta)$ and $J_z^{(2)}(\phi)$ is not retained for all $N$.

Figures 9–11 present the quantum predictions of the

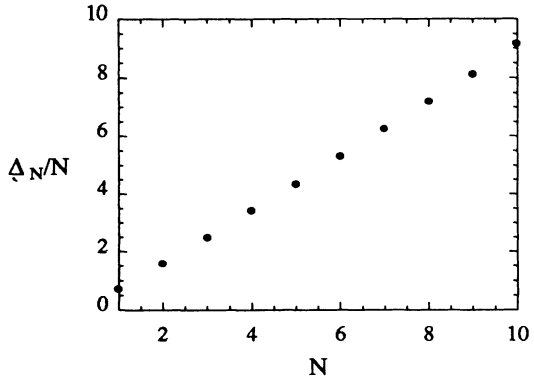


FIG. 9. Plot of the maximum violation ($\Delta_N$) of Mermin's higher-spin inequality for the two mode state $|N\rangle_1|N\rangle_2$. A violation of the inequality occurs for $\Delta_N > 0$. The same results occur in both the polarizer and phase-shifter–beam-splitter arrangements (the angles are chosen for each $N$ to maximize the violation).

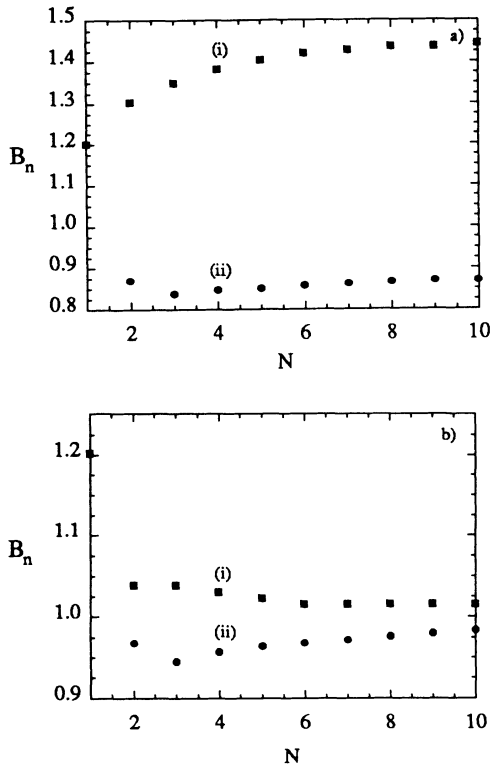


FIG. 10. Plot of the maximum violation of the Clauser-Horne Bell inequality. $B_n$ versus $N$, the number of photons in the correlated two-mode state $|N\rangle_1|N\rangle_2$, for (a) the polarizer arrangement with (i) $n = N$ and (ii) $n = N-1$ and (b) the phase-shifter–beam-splitter arrangement with (i) $n = N$ and (ii) $n = N-1$. A violation of the inequality occurs for $B_n > 1$ (the angles are chosen for each $N$ to maximize the violation).

state (3.12) for the weaker versions of the various classical expressions (2.4), (2.7), and (2.10). Here we again observe a clear violation of all the different types of Bell inequalities discussed for $N = n$. However, in both the Clauser-Horne inequality (2.7) and the product inequality (2.10) no violation is seen for $n < N$ (that is, when fewer than $N$ photons are detected at $C$ and $D$, where $N$ is the number of photons incident at both $A_1$ and $B_1$). We have previously [11] presented and discussed the predictions for the Clauser-Horne inequality using polarizers [Fig. 10(a)].

The calculations presented model two sets of $N$ quanta simultaneously incident on the beam splitters of the apparatus depicted. The need for simultaneity in order to obtain the violation is apparent when we examine the $N = 1$ case. Let us consider the arrangements of the type shown in Figs. 6–8. We consider the ensemble where a single photon is detected at both sets of detectors $C$ and $D$. The state (3.13) is a superposition of two states, the first where the photon detected at $C$ comes from $A_1$ (the signal field) and the second where the photon at $C$ comes from $B_1$ (the idler field). With the introduction of a sufficient time delay between the incident signal and idler

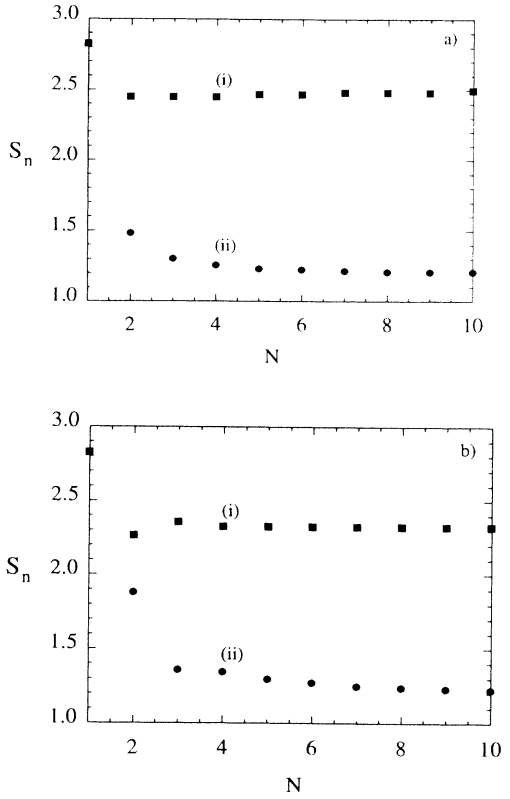


FIG. 11. Plot of the maximum violation of the product Bell inequality. $S_n$ versus $N$, the number of photons in the correlated two-mode state $|N\rangle_1|N\rangle_2$, for (a) the polarizer arrangement with (i) $n = N$ and (ii) $n = N - 1$ and (b) the phase-shifter–beam-splitter arrangement with (i) $n = N$ and (ii) $n = N - 1$. A violation of the inequality occurs for $S_n > 2$ (the angles are chosen for each $N$ to maximize the violation).

photons the origin of a particular photon may be inferred. Hence the superposition nature of the state is lost and no violations of the classical predictions will be possible. The parametric down-conversion process generates fields with the required correlated photon arrival times [5].

## IV. GENERATION OF THE HIGHER-SPIN CORRELATED QUANTUM STATES USING PARAMETRIC DOWN-CONVERSION

Correlated photon-number states of the type we have been considering can be generated using down-conversion [11,12]. We model the process in simple terms by the following Hamiltonian representing pair generation from a nondepleting classical pump field of amplitude $\epsilon$ and frequency $\omega_3$:

$$H = -\hbar\chi\epsilon\left(a_1 b_1 + a_1^\dagger b_1^\dagger\right). \tag{4.1}$$

Here the $a_1, b_1$ are the boson operators for orthogonal signal and idler modes of frequency $\omega_1, \omega_2$, respectively, such that $\omega_3 = \omega_1 + \omega_2$. The $\chi$ is proportional to the susceptibility of the medium. This Hamiltonian incorporates only single modes and hence it will usually apply where the interaction takes place inside a cavity. The model has also been used by Smithey *et al.* [16] to explain experimentally observed photon-number correlations in usual nondegenerate parametric down-conversion with no cavity. The orthogonal fields may be spatially separated. The state generated after an interaction time $t$ is

$$\sum_{N=0}^{\infty} c_N |N\rangle|N\rangle, \tag{4.2}$$

where

$$c_N = \frac{[-i\tanh r]^N}{\cosh r} \tag{4.3}$$

with $r = \chi\epsilon t$. Here we observe that because the signal and idler are generated in pairs, there is a correlation between the signal and idler photon number. Thus we have a method for generating correlated number states with $N > 1$.

We consider also the twin parametric down-conversion process

$$H = \kappa\left(a_+ b_+ + a_- b_-\right) + \kappa^*\left(a_+^\dagger b_+^\dagger + a_-^\dagger b_-^\dagger\right), \tag{4.4}$$

where the entangled states are produced more directly. Here the pairs $a_+, b_+$ and $a_-, b_-$ may represent down-converted photon pairs of differing $k$ vectors or different frequencies. The $a_\pm, b_\pm$ here are the inputs to the experimental arrangements considered in Figs. 1 and 2. The advantage of using the four-mode interaction is that it potentially allows a strong test of the Bell inequalities, as compared to the arrangements depicted in Figs. 6–11, where, as discussed above, auxiliary assumptions are necessary in deriving the Bell inequalities. The experiment of Rarity and Tapster [8] uses parametric amplification in this manner to produce the $N = 1$ entangled state of III and uses the beam-splitter phase-shifter arrangement of Fig. 2 to show a violation of Bell's inequality. Violation of Bell's inequality using such a twin beam was predicted by Reid and Walls [21,24]. The state generated after an interaction time $t$ is

$$|\Psi\rangle = \sum_{N=0}^{\infty} \bar{c}_N \sum_{m=0}^{N} |m\rangle_{a_+}|N-m\rangle_{a_-}|m\rangle_{b_+}|N-m\rangle_{b_-}, \tag{4.5}$$

where

$$\bar{c}_N = \frac{[-i\tanh r]^N}{\cosh^2 r}. \tag{4.6}$$

Assuming initially that the signal and idler may be extracted from the cavity to maintain the correlation given in (4.2) for the two-mode system [or (4.5) for the four-mode system], we observe that we require near perfect photodetection efficiency in order to obtain precisely the violations plotted in Figs. 4 and 5 for the four-mode arrangement and Figs. 10 and 11 for the two-mode system, for all $r$ values. The perfect detection allows one to determine precisely the value of $N$, the number of photons incident on each apparatus provided one has beam

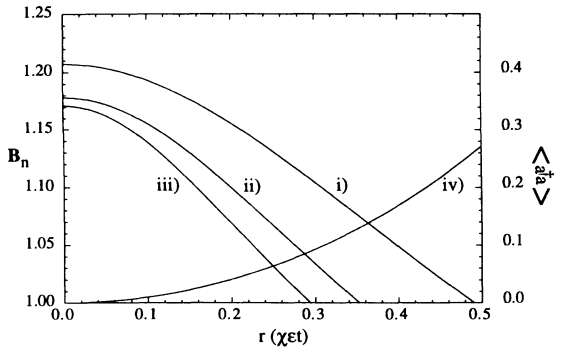


FIG. 12. Plot of the maximum violation of the Clauser-Horne Bell inequality using four-mode parametric down-conversion in the low efficiency limit. $B_n$ versus $r$ $(\chi\epsilon t)$ for (i) $n = 1$, (ii) $n = 2$, and (iii) $n = 3$. Curve (iv) is the mean photon number $\langle a_+^\dagger a_+ \rangle$. The same results occur for both the polarizer and phase-shifter arrangements. A violation of the inequality occurs for $B_n > 1$ (the angles are chosen for each $n$ to maximize the violation).

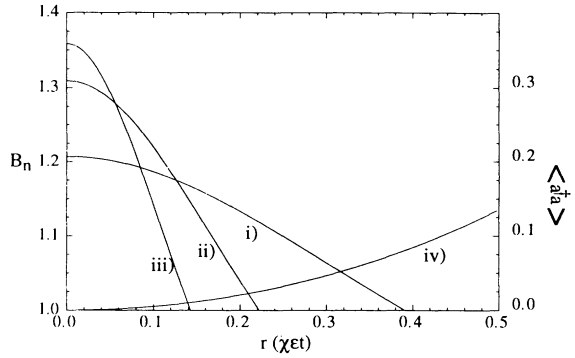


FIG. 13. Plot of the maximum violation of the Clauser-Horne Bell inequality using two-mode parametric down-conversion in the low efficiency limit. $B_n$ versus $r$ $(\chi\epsilon t)$ for (i) $n = 1$, (ii) $n = 2$, and (iii) $n = 3$. Curve (iv) is the mean photon number $\langle a_+^\dagger a_+ \rangle$. These results are for the polarizer arrangements. A violation of the inequality occurs for $B_n > 1$ (the angles are chosen for each $n$ to maximize the violation).

splitters or double-sided polarizers so that one can detect photons at all of the locations $C_+$, $C_-$, $D_+$, and $D_-$. One can then in principle restrict measurements to the subensemble where a total of $N$ photons are incident at each analyzer. In the Clauser-Horne-type experiment, one would need to add detectors at $C_-$ and $D_-$. The predictions for this experiment in the limit of low detection efficiency without detectors at the $C_-$ and $D_-$ positions have been presented by us previously [11] and are shown in Fig. 12 for the four-mode arrangement and in Fig. 13 for the two-mode arrangement. Derivation of the Bell-type inequalities in this low-efficiency case requires an extension of the usual auxiliary assumption and is discussed in Sec. VI. Detection of a total of $n$ quanta at both locations $C$ and $D$ by inefficient detectors leaves open the possibility that the input state may have been $n+1$ photons or higher and the state $|n+k\rangle|n+k\rangle$ $(k > 0)$ contributes to the probability $P_n(\theta,\phi)$, giving results different from those predicted in Figs. 4, 5, 10, and 11. Figures 4, 5, 10, and 11 show, for both the Clauser-Horne and product cases, a loss of the violation of the various Bell's inequalities, where $n = N-1$, indicating detection loss to be an important effect and particularly relevant where one has poor detector efficiencies.

To calculate this effect, we need to evaluate the appropriate joint probabilities for detection of photons at the four locations. The photon counting probabilities may be expressed in terms of the moments of $c_+$, $c_-$, $d_+$, and $d_-$ by applying the usual photon counting formula derived by Keller and Kleiner [26]. The probability of detecting $N$ photons at $C_+$, 0 photons at $C_-$, $N$ photons at $D_+$, and 0 photons at $D_-$ is

$$P_{N,0,N,0}(\theta,\phi) = \eta^{2N}\Big\langle : \Big\{ \Big(c_+^\dagger c_+ d_+^\dagger d_+\Big)^N \times \exp\Big[-\eta\Big(c_+^\dagger c_+ + c_-^\dagger c_- + d_+^\dagger d_+ + d_-^\dagger d_-\Big)\Big]\Big\} : \Big\rangle \tag{4.7}$$

while the probability $P_{N,0,N}(\theta,-)$ of detecting $N$ photons at $C_+$, 0 photons at $C_-$, and $N$ photons at $D$ with the polarizer removed is

$$P_{N,0,N}(\theta,-) = \eta^{2N}\Big\langle : \Big\{ \Big(c_+^\dagger c_+\Big)^N \Big(d_+^\dagger d_+ + d_-^\dagger d_-\Big)^N \times \exp\Big[-\eta\Big(c_+^\dagger c_+ + c_-^\dagger c_- + d_+^\dagger d_+ + d_-^\dagger d_-\Big)\Big]\Big\} : \Big\rangle. \tag{4.8}$$

Here $\eta$ is the quantum efficiency of the detector. For the product system we can write the appropriate correlation function $E_N(\theta,\phi)$ (where we detect a total of $N$ photons at $C$ and a total of $N$ photons at $D$) as

$$E_N(\theta,\phi) = \frac{\Big\langle : \Big\{ \Big(c_+^\dagger c_+ - c_-^\dagger c_-\Big)^N \Big(d_+^\dagger d_+ - d_-^\dagger d_-\Big)^N \exp\Big[-\eta\Big(c_+^\dagger c_+ + c_-^\dagger c_- + d_+^\dagger d_+ + d_-^\dagger d_-\Big)\Big]\Big\} : \Big\rangle}{\Big\langle : \Big\{ \Big(c_+^\dagger c_+ + c_-^\dagger c_-\Big)^N \Big(d_+^\dagger d_+ + d_-^\dagger d_-\Big)^N \exp\Big[-\eta\Big(c_+^\dagger c_+ + c_-^\dagger c_- + d_+^\dagger d_+ + d_-^\dagger d_-\Big)\Big]\Big\} : \Big\rangle}. \tag{4.9}$$

It is readily shown (see Sec. VI) that the $P_{N,0,N,0}(\theta,\phi)$, $P_{N,0,N}(\theta,-)$, and $E_N(\theta,\phi)$ obey the inequalities (2.7) and (2.10), substituting for $P_n(\theta,\phi)$, $P_n(\theta,-)$ and $E_n(\theta,\phi)$, respectively. This is provided the auxiliary assumption discussed in Sec. VI is made.

The results obtained upon evaluating $B_N$ for various efficiencies are plotted in Fig. 14 for the Clauser-Horne inequality with the four-mode parametric interaction (here

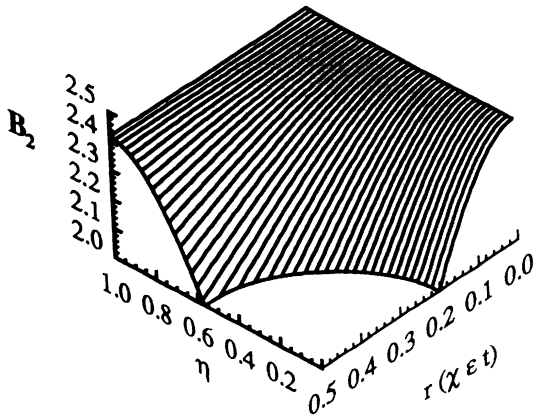


FIG. 14. Plot of the maximum violation of the Clauser-Horne Bell inequality using four-mode parametric down-conversion. $B_2$ versus $r$ ($\chi\epsilon t$), with varying photodetection efficiency $\eta$ for (a) the polarizer arrangement (angles chosen such that $\varphi = \theta - \phi = \theta' - \phi = \theta' - \phi' = (\theta - \phi')/3$=0.277) and (b) the phase-shifter–beam-splitter arrangement (angles chosen such that $\varphi$=2.586). A violation of the inequality occurs for $B_2 > 1$. The same results occur in the polarizer and phase-shifter–beam-splitter arrangements.

one has additional detectors at $C_-$ and $D_-$), in Fig. 15 for the product inequality with the four-mode parametric interaction, in Fig. 16 for the Clauser-Horne inequality with the two-mode interaction, and in Fig. 17 for the product inequality. Where the loss is significant a violation of Bell's inequality is obtained only for fields where the probability of higher photon-number states being generated is negligible. For the parametric solution (4.2) and (4.5) this requires us to operate at low intensities. Unfortunately this reduces the probability of actually detecting $N$ photons at each set of detection apparatus (whether it be $N$ photons at $C_+, D_+$ for the Clauser-Horne inequality or $N$ photons at $C, D$ for the product inequality), making the experiment difficult for large $N$. In this limit of small $\eta$ we are required in the two-mode parametric case, in order to obtain a violation of the $N = 2$ inequality, to operate in a regime where the probability of the two-photon state is $\frac{1}{20}$ that of the one-photon state. This result has been discussed by us previously [11,12] for the two-mode interaction. The results in this low detection efficiency limit are not so much improved by the additional detectors suggested in the Clauser-Horne case. This is because in the low intensity regime, the probability of states with higher photon numbers is very small. We note, however, that the weaker Clauser-Horne inequality [where the marginal probability in (2.7) is replaced by a joint probability] will not be applicable in the higher r regime without the use of the additional detectors at $C_-$ and $D_-$, since the auxiliary assumption will break down in this case (this is discussed in Sec. VI).

Higher detection efficiencies allow violation of Bell's inequality for greater values of $r$, proportional to the pump intensity and the parametric interaction time. For higher $r$ values, the mean intensities of the signal and idler fields becomes greater. Violation of the $N$th-order inequalities is predicted in this regime. However, while the average photon number may be high, the parametric down-conversion with a classical nondepleting pump as modeled here by (4.1) and (4.4) has a super-Poissonian photon-number distribution for the signal and idler fields. This means that the probability of actually detecting pre-

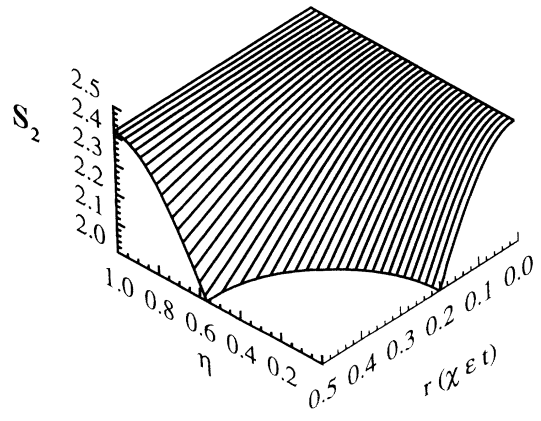


FIG. 15. Plot of the maximum violation of the product Bell inequality using four-mode parametric down-conversion. $S_2$ versus $r$ ($\chi\epsilon t$), with varying photodetection efficiency $\eta$ for (a) the polarizer arrangement [angles chosen such that $\varphi = \theta - \phi = \theta' - \phi = \theta' - \phi' = (\theta - \phi')/3$=0.3925] and (b) the phase-shifter–beam-splitter arrangement (angles chosen such that $\varphi$=2.749). A violation of the inequality occurs for $S_2 > 2$. The same results occur in the polarizer and phase-shifter–beam-splitter arrangements.

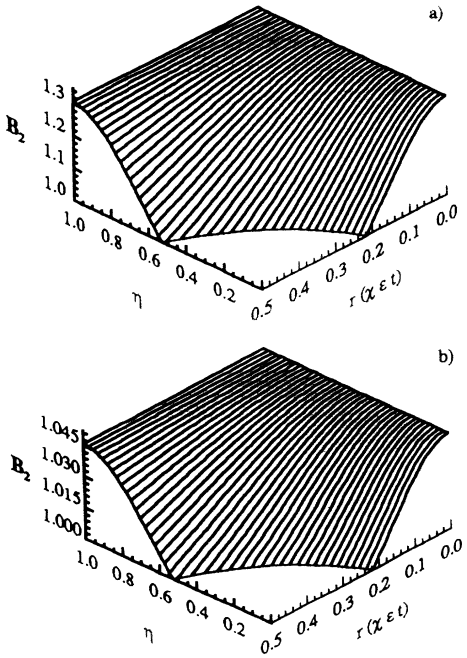


FIG. 16. Plot of the maximum violation of the Clauser-Horne Bell inequality using two-mode parametric down-conversion. $B_2$ versus $r$ ($\chi\epsilon t$), with varying photodetection efficiency $\eta$ for (a) the polarizer arrangement (angles chosen are $\theta = 0.365$, $\theta' = 3.050$, $\phi = -1.662$, and $\phi' = 1.955$) and (b) the phase-shifter–beam-splitter arrangement [angles are chosen such that $\varphi = \theta - \phi = \theta' - \phi = \theta' - \phi' = (\theta - \phi')/3 = 0.627$]. A violation of the inequality occurs for $B_2 > 1$.

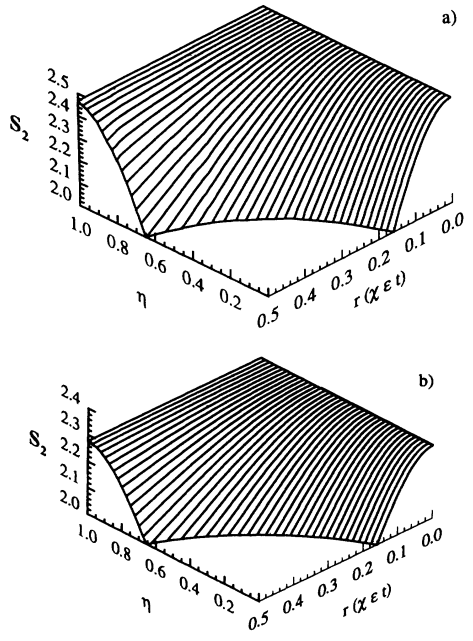


FIG. 17. Plot of the maximum violation of the product Bell inequality using parametric down-conversion. $S_2$ versus $r$ ($\chi\epsilon t$), with varying photodetection efficiency $\eta$ for (a) the polarizer arrangement (angles chosen are $\theta = 1.290$, $\theta' = 0.666$, $\phi = 0.522$, and $\phi' = 1.443$) and (b) the phase-shifter–beam-splitter arrangement [angles are chosen such that $\varphi = \theta - \phi = \theta' - \phi = \theta' - \phi' = (\theta - \phi')/3 = 0.393$]. A violation of the inequality occurs for $S_2 > 2$.

cisely $N$ photons at $C$ and $D$ will be small. Also, because we consider here the reduced ensemble, auxiliary assumptions are used, making a strong test of Bell inequalities not possible, even in the high detection efficiency limit.

## V. GENERATION OF THE HIGHER-SPIN CORRELATED QUANTUM STATES USING PARAMETRIC OSCILLATION

The correlated photon-number states of the type (3.1) and $|N\rangle|N\rangle$ have been generated for $N = 1$ using parametric down-conversion [6–9,16]. Generation of the $N$ quanta wave packet using parametric down-conversion is made difficult because of the poor conversion efficiency of pump to signal photons. One possibility might be to improve the efficiency by employing nondegenerate parametric oscillation where the parametric process takes place inside a cavity. One can resonate the cavity to two orthogonal signal and idler modes so that the parametric oscillation is modeled by the Hamiltonian

$$H = i\hbar\epsilon\left(c^\dagger - c\right) + i\hbar g\left(ca^\dagger b^\dagger - c^\dagger ab\right) + \sum_i \left(a_i^\dagger \Gamma_{Ri} + a_i \Gamma_{Ri}^\dagger\right). \tag{5.1}$$

Alternatively, we could consider four resonant signal and idler modes

$$\begin{aligned} H = {} & i\hbar\epsilon\left(c^\dagger - c\right) \\ & + i\hbar g\left[c\left(a_+^\dagger b_+^\dagger + a_-^\dagger b_-^\dagger\right) - c^\dagger\left(a_+ b_+ + a_- b_-\right)\right] \\ & + \sum_i \left[a_{i_+}^\dagger \Gamma_{Ri_+} + a_{i_-}^\dagger \Gamma_{Ri_-}\right] \\ & + \sum_i \left[a_{i_+} \Gamma_{Ri_+}^\dagger + a_{i_-} \Gamma_{Ri_-}^\dagger\right] \end{aligned} \tag{5.2}$$

as a means of generating the four-mode state originally considered by Drummond [10]. Here $\epsilon$ is proportional to the classical pump amplitude. The modes $c$, $a$, and $b$ are the pump, signal, and idler modes at the frequencies $\omega_1 + \omega_2$, $\omega_1$, and $\omega_2$, respectively. We also use the notation $a = a_1$, $b = a_2$, and $c = a_3$ for convenience. The loss of the field $a_i$ through the cavity mirrors is modeled by the coupling to an external reservoir $\Gamma_{Ri}$. It is the field external to the cavity that is measurable and of interest to us here. We consider the situation where losses occur through just one of the cavity mirrors and denote the signal and idler fields transmitted through it by $a_{\rm ext}$ and $b_{\rm ext}$, respectively. The cavity photon loss rate is assumed to be equal for signal and idler and is denoted by $2\kappa$. The external operators are related to the internal $a$ and $b$ operators by the boundary condition at the cavity mirror. The model describing the interaction involving four cavity modes has been studied previously by Graham [27] and Reid and Walls [21].

### A. The four-mode system

We present calculations for this case because the use of the four-mode as compared to the two-mode system may allow one to test at least in principle the stronger original form of Bell's inequalities. In order to evaluate the quantum predictions for the classical inequalities (2.4)–(2.10) we consider the configurations discussed in II and require the calculation of joint probabilities such as that for detecting $n_1$ photons at $C_+$ and $n_2$ photons at $D_+$, in a particular detection time. The input fields denoted by $a_+, b_+$ in Figs. 1 and 2 are now replaced by the external fields $a_{+\,\rm ext}, b_{+\,\rm ext}$. We will consider here only the situation where the photon detection time is much shorter than the field coherence time. Our initial objective is to demonstrate the possibility of obtaining violations of Bell's inequalities using correlated states generated via cavity configurations [24]. For detection times much shorter than the field coherence time the probabilities are directly proportional to the normally ordered correlation functions of the field. Thus, for example, the probability of detecting $n_1$ photons at $C_+$ and $n_2$ photons at $D_+$ is given by

$$P(m_1(\theta), m_2(\phi)) \sim \langle : c_{+\rm ext}^{\dagger\, n_1} c_{+\rm ext}^{n_1} d_{+\rm ext}^{\dagger\, n_2} d_{+\rm ext}^{n_2} : \rangle, \tag{5.3}$$

where

$$n_1 = m_1(\theta) + N/2, \tag{5.4}$$

$$n_2 = m_2(\phi) + N/2. \tag{5.5}$$

The constant of proportionality is $(\eta T)^{n_1+n_2}$, the effec-

tive detection efficiency factor, taken here to be small. Here the $c_{\pm\,\mathrm{ext}}, d_{\pm\,\mathrm{ext}}$ are defined in terms of the external signal and idler fields $a_{\pm\,\mathrm{ext}}$ and $b_{\pm\,\mathrm{ext}}$ in accordance with the transformations (2.1) or (2.2). The detection time $T$ is assumed here to be short so that the $n_1$ and $n_2$ quanta are detected simultaneously on the time scale of the passage time for the photons through the beam-splitter–polarizer or interferometric apparatus.

In order to test the classical inequalities for a fixed value of spin $N/2$, we focus attention on situations where a total of $N$ quanta are incident and detected at both locations $C$ and $D$. Because we consider here a low efficiency limit, it becomes necessary in practice to consider the weaker versions of the classical inequalities, where we only record events for the subensemble where $N$ photons are detected at both $C$ and $D$. Thus we require the calculation of the probability of detecting $n_1$ photons at $c_+$, $N-n_1$ photons at $c_-$, $n_2$ photons at $D_+$, and $N-n_2$ photons at $D_-$. The probability $P_N(\theta,\phi)$ defined for the Clauser-Horne-type inequality (2.7) becomes

$$P_N(\theta,\phi)=\frac{\langle: c_{+\mathrm{ext}}^{\dagger\,N} c_{+\mathrm{ext}}^{N} d_{+\mathrm{ext}}^{\dagger\,N} d_{+\mathrm{ext}}^{N} :\rangle}{\langle: [c_{+\mathrm{ext}}^{\dagger} c_{+\mathrm{ext}}+c_{-\mathrm{ext}}^{\dagger} c_{-\mathrm{ext}}]^N [d_{+\mathrm{ext}}^{\dagger} d_{+\mathrm{ext}}+d_{-\mathrm{ext}}^{\dagger} d_{-\mathrm{ext}}]^N :\rangle}. \tag{5.6}$$

The "marginal" probability defined in the inequality becomes

$$P_N(\theta,-)=\frac{\langle: c_{+\mathrm{ext}}^{\dagger\,N} c_{+\mathrm{ext}}^{N} [d_{+\mathrm{ext}}^{\dagger} d_{+\mathrm{ext}}+d_{-\mathrm{ext}}^{\dagger} d_{-\mathrm{ext}}]^N :\rangle}{\langle: [c_{+\mathrm{ext}}^{\dagger} c_{+\mathrm{ext}}+c_{-\mathrm{ext}}^{\dagger} c_{-\mathrm{ext}}]^N [d_{+\mathrm{ext}}^{\dagger} d_{+\mathrm{ext}}+d_{-\mathrm{ext}}^{\dagger} d_{-\mathrm{ext}}]^N :\rangle}. \tag{5.7}$$

The spin-product expectation value defined for inequality (2.10) becomes

$$E_N(\theta,\phi)=\frac{\langle: [c_{+\mathrm{ext}}^{\dagger} c_{+\mathrm{ext}}-c_{-\mathrm{ext}}^{\dagger} c_{-\mathrm{ext}}]^N [d_{+\mathrm{ext}}^{\dagger} d_{+\mathrm{ext}}-d_{-\mathrm{ext}}^{\dagger} d_{-\mathrm{ext}}]^N :\rangle}{\langle: [c_{+\mathrm{ext}}^{\dagger} c_{+\mathrm{ext}}+c_{-\mathrm{ext}}^{\dagger} c_{-\mathrm{ext}}]^N [d_{+\mathrm{ext}}^{\dagger} d_{+\mathrm{ext}}+d_{-\mathrm{ext}}^{\dagger} d_{-\mathrm{ext}}]^N :\rangle}. \tag{5.8}$$

The moments required are directly related through the transformations (2.1) and (2.2) to moments involving the external flux operators $a_{\pm\,\mathrm{ext}}$ and $b_{\pm\,\mathrm{ext}}$. The correlation functions for the external operators are related to those of the cavity modes $a_\pm$ and $b_\pm$ as determined by the cavity boundary condition. This has been considered previously [28] and one obtains relations such as

$$\langle: a_{\mathrm{ext}}^{\dagger i} a_{\mathrm{ext}}^{j} b_{\mathrm{ext}}^{\dagger k} b_{\mathrm{ext}}^{l} :\rangle = (2\kappa)^{\frac{i+j+k+l}{2}} \langle: a^{\dagger i} a^{j} b^{\dagger k} b^{l} :\rangle. \tag{5.9}$$

The normally ordered moments are directly related through the constant of proportionality which is the appropriate power of $\sqrt{2\kappa}$. The cavity moments have been derived previously [21] for the case where $\kappa_3 \gg \kappa$, where $\kappa_3$ is the cavity loss rate for the pump mode $c$. The approach used was to derive a Fokker-Planck equation for the generalized $P$ representation [29] of the density operator

$$\hat{\rho}=\int P\left[\left(\alpha_i^{\dagger},\alpha_i\right)\right] \frac{|\,(\alpha_i)\rangle\left\langle\left(\alpha_i^{\dagger}\right)\right|}{\left\langle\left(\alpha_i^{\dagger}\right)\middle|(\alpha_i)\right\rangle} d\mu. \tag{5.10}$$

Here $|\,(\alpha_i)\rangle = |\alpha_+\rangle|\alpha_-\rangle|\beta_+\rangle|\beta_-\rangle$ and $d\mu$ is an integration measure. Here $\alpha_\pm, \alpha_\pm^{\dagger}, \beta_\pm, \beta_\pm^{\dagger}$ are $c$ numbers corresponding to operators $a_\pm, a_\pm^{\dagger}, b_\pm, b_\pm^{\dagger}$, respectively. The $\alpha_i$ and $\alpha_i^{\dagger}$ are independent complex variables. The equation for $P\left[\left(\alpha_i^{\dagger},\alpha_i\right)\right]$ is derived using standard methods from the master equation for the density operator. The Fokker-Planck equation is equivalent to the following $c$-number equations in the stochastic amplitudes, where the pump has been eliminated adiabatically

$$\dot{\alpha}_+ = -\kappa\alpha_+ + \frac{g\beta_+^{\dagger}}{\kappa_3}\left[\epsilon - g\alpha_+\beta_+ - g\alpha_-\beta_-\right] + F_{\alpha_+}(t), \tag{5.11}$$

$$\dot{\beta}_+ = -\kappa\beta_+ + \frac{g\alpha_+^{\dagger}}{\kappa_3}\left[\epsilon - g\alpha_+\beta_+ - g\alpha_-\beta_-\right] + F_{\beta_+}(t). \tag{5.12}$$

The equations for $\alpha_+^{\dagger}$ and $\beta_+^{\dagger}$ are obtained by exchanging $\alpha_\pm$ and $\alpha_\pm^{\dagger}$, and $\beta_\pm$ and $\beta_\pm^{\dagger}$, and taking the complex conjugate of the other terms. Similarly the equations for $\alpha_-$, $\beta_-$, $\alpha_-^{\dagger}$, and $\beta_-^{\dagger}$ are obtained by exchanging $\alpha_+$ and $\alpha_-$, $\beta_+$ and $\beta_-$, $\alpha_+^{\dagger}$ and $\alpha_-^{\dagger}$, and $\beta_+^{\dagger}$ and $\beta_-^{\dagger}$. The nonzero noise correlations are

$$\langle F_{\alpha_\pm}(t) F_{\beta_\pm}(t')\rangle = g\epsilon\delta(t-t'), \tag{5.13}$$

$$\langle F_{\alpha_\pm^{\dagger}}(t) F_{\beta_\pm^{\dagger}}(t')\rangle = g\epsilon^{*}\delta(t-t'). \tag{5.14}$$

Reid and Walls [21] derived a potential solution for $P$ in the steady state. An appropriate contour of integration was defined. Normally ordered moments are calculated directly by integrating over the $P$ solution. For example,

$$\langle: a_+^{\dagger\,N} a_+^{N} b_+^{\dagger\,N} b_+^{N} :\rangle = \int P\left(\left[\alpha_i^{\dagger},\alpha_i\right]\right) \alpha_+^{\dagger\,N}\alpha_+^{N}\beta_+^{\dagger\,N}\beta_+^{N} d\mu. \tag{5.15}$$

The stochastic equations reduce to the classical equations if one ignores the quantum noise terms and uses $\alpha_i^{\dagger} = \alpha_i^{*}$. The classical threshold condition is readily derived by examining the steady-state solutions for the classical amplitudes. Here $g\epsilon/\kappa_3\kappa = 1$ corresponds to threshold.

Here we are concerned only with the system operating below threshold where the classical steady-state solution is $\alpha_+ = \alpha_- = \beta_+ = \beta_- = 0$.

In all current experiments the threshold photon number is very large and the effect of the quantum noise is to perturb about the classical solutions. In this limit, predictions may be obtained from a linearization of the fluctuations. One may choose to linearize operator equations derived directly from (5.2) or to linearize the stochastic equations (5.11) and (5.12). It is particularly convenient to note that [as is the case with the state (3.2)] the equations are invariant under rotations of the stochastic variables $\alpha_\pm$ and $\beta_\pm$ to the new variables $c_\pm$ and $d_\pm$

$$\begin{aligned} c_+ &= \alpha_+ \cos\theta + \alpha_- \sin\theta, \\ c_- &= -\alpha_+ \sin\theta + \alpha_- \cos\theta, \\ d_+ &= \beta_+ \cos\theta + \beta_- \sin\theta, \\ d_- &= -\beta_+ \sin\theta + \beta_- \cos\theta. \end{aligned} \tag{5.16}$$

The stochastic variables $c_\pm, d_\pm$ determine directly the moments of the measured $c_{\pm_{\rm ext}}$ and $d_{\pm_{\rm ext}}$ fields in accordance with the relation of the type (5.3). Thus it is convenient to rotate the $\alpha_\pm$ and $\beta_\pm$ by $\theta$, the angle determined by the measurement made at $C$. One then evaluates the prediction of $P_N(\theta,\phi)$ by considering correlations of the type $\langle : c_+^{\dagger N} c_+^N d_+^{\dagger N} d_+^N : \rangle$, where

$$\begin{aligned} c_+ &= \alpha_+, \\ c_- &= \alpha_-, \\ d_+ &= \beta_+ \cos\varphi + \beta_- \sin\varphi, \\ d_- &= -\beta_+ \sin\varphi + \beta_- \cos\varphi, \end{aligned} \tag{5.17}$$

and here $\varphi = \phi - \theta$. Figure 18 depicts the violation of the classical inequality (2.7), for $N = 1$ and 2, while Fig. 19 depicts the results for the product inequality (2.10). Here we have used linearized solutions.

### B. The two-mode results

So far we have investigated the four-mode results. It is also possible to do the two-mode calculation. Using a procedure similar to that used before, we can write down the following $c$ number equations:

$$\dot{\alpha} = -\kappa\alpha + \frac{g\beta^\dagger}{\kappa_3}[\epsilon - g\alpha\beta] + F_\alpha(t), \tag{5.18}$$

$$\dot{\beta} = -\kappa\beta + \frac{g\alpha^\dagger}{\kappa_3}[\epsilon - g\alpha\beta] + F_\beta(t). \tag{5.19}$$

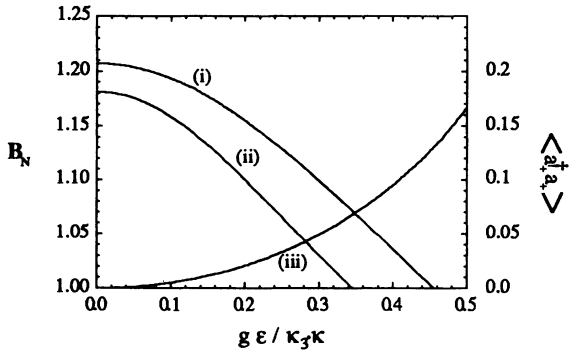


FIG. 18. Plot of the violation of the four-mode Clauser-Horne Bell inequality. $B_N$ versus $g\epsilon/\kappa_3\kappa$ for parametric oscillation. Here $\kappa_3/\kappa = 10$. (i) $N = 1$ and (ii) $N = 2$. Curve (iii) is the mean photon number $\langle a_+^\dagger a_+ \rangle$. The same results occur for both the polarizer and phase-shifter arrangements. A violation of the inequality occurs for $B_N > 1$ (the angles are chosen for each $N$ to maximize the violation).

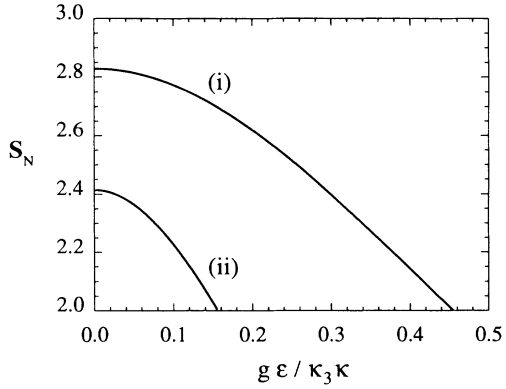


FIG. 19. Plot of the violation of the four-mode product Bell inequality. $S_N$ versus $g\epsilon/\kappa_3\kappa$ for parametric oscillation. Here $\kappa_3/\kappa = 10$. (i) $N = 1$ and (ii) $N = 2$. The same results occur for both the polarizer and phase-shifter arrangements. A violation of the inequality occurs for $S_N > 2$ (the angles are chosen for each $N$ to maximize the violation).

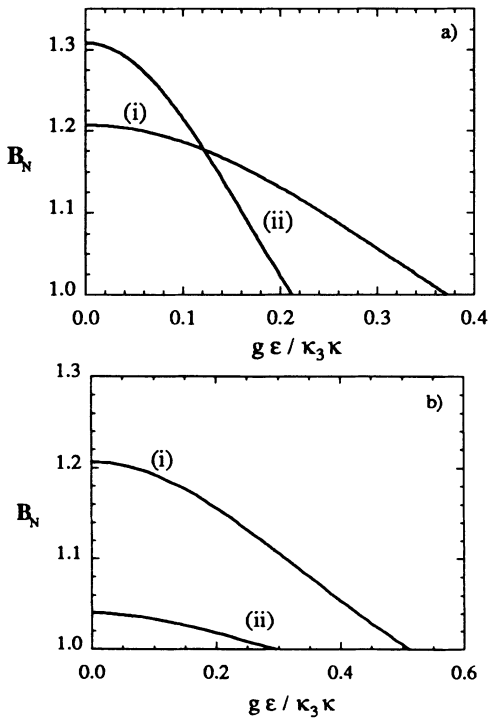


FIG. 20. Plot of the violation of the two-mode Clauser-Horne Bell inequality. $B_N$ versus $g\epsilon/\kappa_3\kappa$ for parametric oscillation. Here $\kappa_3/\kappa = 10$. (a) The polarizer arrangement with (i) $N = 1$ and (ii) $N = 2$. (b) the phase-shifter–beam-splitter arrangement with (i) $N = 1$ and (ii) $N = 2$. A violation of the inequality occurs for $B_N > 1$ (the angles are chosen for each $N$ to maximize the violation).

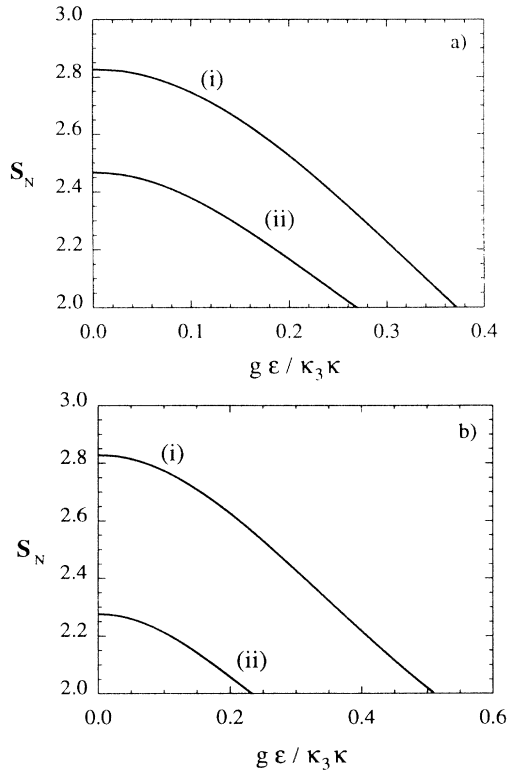


FIG. 21. Plot of the violation of the two-mode product Bell inequality. $S_N$ versus $g\epsilon/\kappa_3\kappa$ for parametric oscillation. Here $\kappa_3/\kappa = 10$. (a) The polarizer arrangement with (i) $N = 1$ and (ii) $N = 2$. (b) The phase-shifter–beam-splitter arrangement with (i) $N = 1$ and (ii) $N = 2$. A violation of the inequality occurs for $S_N > 2$ (the angles are chosen for each $N$ to maximize the violation).

The equations for $\alpha^\dagger$ and $\beta^\dagger$ are obtained by exchanging $\alpha$ and $\alpha^\dagger$, and $\beta$ and $\beta^\dagger$, and taking the complex conjugate of the other terms. The nonzero noise correlations are

$$\langle F_\alpha(t)F_\beta(t')\rangle = g\epsilon\delta(t-t'), \tag{5.20}$$

$$\langle F_{\alpha^\dagger}(t)F_{\beta^\dagger}(t')\rangle = g\epsilon^*\delta(t-t'). \tag{5.21}$$

It is then possible to linearize these equations and hence calculate the expectation values and correlation functions needed for the Clauser-Horne and spin product Bell inequality. It is also possible to solve the nonlinear equations in the regime where $\kappa_3 \gg \kappa$ [30]. In Figs. 20 and 21 we present results for the two-mode case, using a linearized analysis. Here $(g\epsilon/\kappa_3\kappa) = 1$ corresponds to threshold.

### C. Discussion

Results for $N = 1$ have been derived previously by Reid and Walls [21] for the four-mode case. It is seen that violation of Bell inequalities is possible only if one operates sufficiently far below threshold. The reason for the loss of violation when at higher pump powers becomes apparent when one considers the following simple model Hamiltonian for the four- or two-mode parametric down-conversion below threshold, where the pump mode is essentially undepleted and may be modeled as a classical pump:

$$H = -\hbar\chi\epsilon\left\{(a_+b_+ + a_-b_-) + \left(a_+^\dagger b_+^\dagger + a_-^\dagger b_-^\dagger\right)\right\}, \tag{5.22}$$

$$H = -\hbar\chi\epsilon\left(ab + a^\dagger b^\dagger\right). \tag{5.23}$$

This model has been discussed above in Sec. IV. For finite $\epsilon$, one generates a superposition of the $N$ quanta states of the type given by (3.1). At low pump powers only the $N = 1$ state contributes significantly and the violation of the inequalities is obtained. As $\epsilon$ increases the higher-$N$ states are more important. Let us suppose we are interested in the $\frac{N_0}{2}$-spin experiment. At higher pump values, the states with $N > N_0$ give a finite contribution to moments such as $\langle : c_+^{\dagger N_0} c_+^{N_0} d_+^{\dagger N_0} d_+^{N_0} : \rangle$. Thus in the situation we examine here of low photon-detection efficiency, these higher-$N$ states contribute to the joint photodetection probabilities. Their effect is to decrease or destroy the violation of the $\frac{N_0}{2}$-spin classical inequality. It is seen from the results for $N_0 = 2$ that the $N_0$ state can be made to dominate and thus to give the violation similar to that predicted by the higher-spin quantum states (3.1) provided the pump amplitude is sufficiently low. In situations where the detection time $T$ is greater and the detection efficiency increased, one would expect to recover results similar to that described in Secs. III and IV.

## VI. DERIVATION OF THE $N$-PARTICLE BELL INEQUALITY

We summarize the derivation of the Clauser-Horne and Clauser-Horne-Shimony-Holt–Bell inequalities used in this paper. The derivations are straightforward extensions of the original derivations [1,2] as pointed out by Drummond [10].

### A. The $N$-particle Clauser-Horne inequality derivation

The set of "hidden" variables, which we will denote collectively by the symbol $\lambda$, is introduced. For given $\lambda$, the values of all observables are specified as the values of appropriate real-valued functions defined over the domain $\Lambda$ of all possible values for the hidden variable. Now denoting the probability density function for the hidden variables in the state $|\psi\rangle$ by $\rho$ we have that $\rho(\lambda)d\lambda$ measures the probability that the collective hidden variable lies in the range $\lambda$ to $\lambda + d\lambda$. The probability density function is normalized such that

$$\int_\Lambda \rho(\lambda)d\lambda = 1. \tag{6.1}$$

Also it is required that

$$\rho(\lambda) \geq 0. \tag{6.2}$$

We now examine the situations described by Figs. 1 and 2. Applying this hidden variable description to the marginal probability $P_N^{(1)}(\theta)$ for detecting a total of $N$ photons at $C_+$, we may write

$$P_N^{(1)}(\theta) = \int_\Lambda P_N^{(1)}(\lambda,\theta)\rho(\lambda)d\lambda, \tag{6.3}$$

where $P_N^{(1)}(\lambda,\theta)$ is the probability given the state described by $\lambda$. Similarly we have

$$P_N^{(2)}(\phi) = \int_\Lambda P_N^{(2)}(\lambda,\phi)\rho(\lambda)d\lambda, \tag{6.4}$$

where $P_N^{(2)}(\phi)$ is the marginal probability for detecting a total of $N$ photons at $D_+$, and $P_N^{(2)}(\lambda,\phi)$ is the probability of detecting $N$ photons $D_+$, given $\lambda$ and $\phi$. The joint probability for simultaneously detecting $N$ photons at both $C_+$ and $D_+$ is

$$P_N^{(12)}(\theta,\phi) = \int_\Lambda P_N^{(12)}(\lambda,\theta,\phi)\rho(\lambda)d\lambda, \tag{6.5}$$

where $P_N^{(12)}(\lambda,\theta,\phi)$ is the probability for detecting $N$ photons at both locations, given $\lambda$, $\theta$ and $\phi$. Mathematically the locality assumption is written

$$P_N^{(12)}(\lambda,\theta,\phi) = P_N^{(1)}(\lambda,\theta)P_N^{(2)}(\lambda,\phi) \tag{6.6}$$

and therefore Eq. (6.5) reduces to

$$P_N^{(12)}(\theta,\phi) = \int_\Lambda P_N^{(1)}(\lambda,\theta)P_N^{(2)}(\lambda,\phi)\rho(\lambda)d\lambda. \tag{6.7}$$

Next we have the following lemma.

*Lemma.* If $x,x',y,y'$ and $X,Y$ are real numbers such that

$$0 \le x, \quad x' \le X, \quad 0 \le y, \quad y' \le Y, \tag{6.8}$$

then the inequality given by

$$0 \ge xy - xy' + x'y + x'y' - x'Y - yX \ge -XY \tag{6.9}$$

holds.

Thus choosing $x = P_N^{(1)}(\lambda,\theta)$, $y = P_N^{(2)}(\lambda,\phi)$, and $X = Y = 1$, we have

$$-1 \le P_N^{(12)}(\lambda,\theta,\phi) - P_N^{(12)}(\lambda,\theta,\phi') + P_N^{(12)}(\lambda,\theta',\phi)$$

$$+P_N^{(12)}(\lambda,\theta',\phi') - P_N^{(1)}(\lambda,\theta') - P_N^{(2)}(\lambda,\phi) \le 0. \tag{6.10}$$

Integrating inequality (6.10) over $\lambda$ with distribution $\rho(\lambda)d\lambda$, the right-hand side of the inequality can be written as

$$B_N = \frac{P_N^{(12)}(\theta,\phi) - P_N^{(12)}(\theta,\phi') + P_N^{(12)}(\theta',\phi) + P_N^{(12)}(\theta',\phi')}{P_N^{(1)}(\theta') + P_N^{(2)}(\phi)} \le 1. \tag{6.11}$$

To date no situation that violates the Clauser-Horne inequality has been experimentally realized because of poor photodetection efficiencies. With an auxiliary assumption [2,17], realizable experiments have been predicted and shown experimentally to yield a violation of Bell's inequality. We consider the apparatus depicted in Figs. 1 and 2, but now select to measure only joint probabilities where a total of $N$ photons are detected at both $C$ and $D$. One measures the joint probability $P_N^{(12)}(\theta,\phi)$ as before and also the one-sided joint probability $P_N^{(12)}(\theta,-)$, which corresponds to the probability of measuring $N$ photons at $C_+$ and $N$ photons at $D$ where the analyzer (polarizer or beam splitter) at $D$ is removed. The $P_N^{(12)}(-,\phi)$ is the joint probability of detecting $N$ photons at $D_+$ and $N$ photons at $C$ with the analyzer at $C$ removed. In terms of a hidden variable theory the one-sided probabilities are written

$$P_N^{(12)}(\theta,-) = \int_\Lambda \rho(\lambda)P_N^{(1)}(\lambda,\theta)P_N^{(2)}(\lambda)d\lambda, \tag{6.12}$$

where the one-sided state described by $\lambda$ has been factorized using the locality assumption and we have defined $P_N^{(2)}(\lambda)$ as the probability of detecting $N$ photons at $D$ with the analyzer at $D$ removed given $\lambda$. One defines $P_N^{(1)}(\lambda)$ as the probability of detecting $N$ photons at $C$ with the analyzer at $C$ removed. Thus

$$P_N^{(12)}(-,\phi) = \int_\Lambda \rho(\lambda)P_N^{(1)}(\lambda)P_N^{(2)}(\lambda,\phi)d\lambda \tag{6.13}$$

and as before

$$P_N^{(12)}(\theta,\phi) = \int_\Lambda \rho(\lambda)P_N^{(1)}(\lambda,\theta)P_N^{(2)}(\lambda,\phi)d\lambda. \tag{6.14}$$

One can now choose [note that $P_N^{(1)}(\lambda)$ and $P_N^{(2)}(\lambda)$ do not depend on $\theta$ and $\phi$]

$$x = \frac{P_N^{(1)}(\lambda,\theta)}{P_N^{(1)}(\lambda)}, \quad y = \frac{P_N^{(2)}(\lambda,\theta)}{P_N^{(2)}(\lambda)} \tag{6.15}$$

and introduce the auxiliary assumption

$$P_N^{(1)}(\lambda,\theta) \le P_N^{(1)}(\lambda), \qquad P_N^{(2)}(\lambda,\theta) \le P_N^{(2)}(\lambda). \tag{6.16}$$

One selects $X = Y = 1$. Thus one can use the lemma to derive the inequality

$$B_N = \frac{P_N(\theta,\phi) - P_N(\theta,\phi') + P_N(\theta',\phi) + P_N(\theta',\phi')}{P_N(\theta',-) + P_N(-,\phi)} \leq 1, \tag{6.17}$$

where the marginal probabilities are replaced by the one-sided joint probabilities. We have dropped the superscripts for simplicity.

The weaker inequality (6.17) derived with the auxiliary assumption (6.16) has been traditionally used where only a single photon pair is emitted from the source at a time and there is a small probability of actually detecting both photons. One can make measurements and inferences only on the detected ensemble. Special care needs to be taken with the auxiliary assumptions in situations of the type considered in Sec. IV. We examine the parametric down-conversion in the regime where $r$ can be large. If attempting to test the $N$-particle inequalities given in (6.17), we measure the joint probability $P_N(\theta,\phi)$ and the one-sided joint probability $P_N(\theta,-)$ where no polarizer is present at $D$. Now in the larger $r$ regime there is a significant probability that more than $N$ photons are emitted by the source in each signal and idler field. Let us imagine $N+1$ photons incident at both of the analyzers at $C$ and $D$. If all photons are detected, this emission will not contribute to the experimenter's measurement of $P_N(\theta,-)$. It will, however, contribute to $P_N(\theta,\phi)$ since it can give a nonzero probability for precisely $N$ photons being detected at $C_+$. The auxiliary assumption (6.16) thus is not reasonable in this case, particularly where higher detection efficiencies are considered. In Sec. VII we consider another situation where the auxiliary assumption (6.16) will not be valid.

In the situations of parametric down-conversion with arbitrary $r$, the Clauser-Horne-type experiment suggested in this paper therefore employs additional detectors at $C_-$ and $D_-$ to select the subensemble where a total of $N$ photons are detected at $C$ and $D$. We consider the derivation of a suitably modified Clauser-Horne inequality. The one-sided probability $P_N^{(12)}(\theta,-)$ in Eqs. (6.12)–(6.17) now becomes $P_{N,0,N}^{(12)}(\theta,-)$, the joint probability of detecting $N$ photons at $D$ (with the analyzer at $D$ removed), $N$ photons at $C_+$, and zero photons at $C_-$. $P_N^{(12)}(-,\phi)$ becomes $P_{N,N,0}^{(12)}(-,\phi)$, the joint probability of detecting $N$ photons at $C$ (with the analyzer at $C$ removed), $N$ photons at $D_+$, and zero photons at $D_-$. The $P_N^{(1)}(\lambda,\theta)$ becomes $P_{N,0}^{(1)}(\lambda,\theta)$, the probability for detecting $N$ photons at $C_+$ and zero photons at $C_-$, given $\lambda$. $P_N^{(2)}(\lambda,\phi)$ becomes $P_{N,0}^{(2)}(\lambda,\phi)$, the probability of detecting $N$ photons at $D_+$ and zero photons at $D_-$, given $\lambda$. The $P_N^{(1)}(\lambda)$ and $P_N^{(2)}(\lambda)$ remain as defined previously. The probability $P_N^{(12)}(\theta,\phi)$ becomes $P_{N,0,N,0}^{(12)}(\theta,\phi)$, the joint probability for detecting $N$ photons at $C_+$, zero photons at $C_-$, $N$ photons at $D_+$, and zero photons at $D_-$. With the auxiliary assumption now being

$$P_{N,0}^{(1)}(\lambda,\theta) \leq P_N^{(1)}(\lambda),$$
$$P_{N,0}^{(2)}(\lambda,\phi) \leq P_N^{(2)}(\lambda), \tag{6.18}$$

the derivation of the following inequality follows:

$$B_N = \frac{P_{N,0,N,0}(\theta,\phi) - P_{N,0,N,0}(\theta,\phi') + P_{N,0,N,0}(\theta',\phi) + P_{N,0,N,0}(\theta',\phi')}{P_{N,0,N}(\theta,-) + P_{N,N,0}(-,\phi)} \leq 1. \tag{6.19}$$

This is the inequality tested in Secs. IV and V. The auxiliary assumption becomes the following: for every $\lambda$, the probability of detecting $N$ photons at $C_+$ and zero photons at $C_-$ is always less than the probability of detecting $N$ photons with the analyzer at $C$ removed (and similarly for $D$). The additional detectors at $C_-$ and $D_-$ make the auxiliary assumption reasonable.

### B. The $N$th-order product Bell inequality derivation

We now derive the $N$th-order product Bell inequality. This is a straightforward generalization of previous proofs of Bell and CHSH [2]. One may write the measured quantity $E_N(\theta,\phi)$ defined in (2.8) and (2.9) in terms of the hidden variables as

$$E_N(\theta,\phi) = \int \rho(\lambda)\, E_N^{(1)}(\lambda,\theta) E_N^{(2)}(\lambda,\phi) d\lambda$$
$$= \int \rho(\lambda) \left\{ P_N^{(1)}(\lambda,\theta) - P_{N-1}^{(1)}(\lambda,\theta) + P_{N-2}^{(1)}(\lambda,\theta) - \cdots \right\} \left\{ P_N^{(2)}(\lambda,\phi) - P_{N-1}^{(2)}(\lambda,\phi) + P_{N-2}^{(2)}(\lambda,\phi) - \cdots \right\} d\lambda, \tag{6.20}$$

where $E_N^{(1)}(\lambda,\theta)$ and $E_N^{(2)}(\lambda,\phi)$ are the products defined in (2.8) at positions $C$ and $D$, respectively, given the state specified by $\lambda$. These products may be defined in terms of the probabilities $P_{N-i}^{(1)}(\lambda,\theta)$ and $P_{N-i}^{(2)}(\lambda,\phi)$, where $i = 0,\ldots,N$. Here $P_{N-i}^{(1)}(\lambda,\theta)$ is the probability of detecting $N-i$ photons at $C_+$ and $i$ photons at $C_-$, given the state specified by $\lambda$. The $P_{N-i}^{(2)}(\lambda,\phi)$ is the probability of detecting $N-i$ photons at $D_+$ and $i$ photons at $D_-$.

given $\lambda$. Since

$$\left|E_N^{(1)}(\lambda,\theta)\right| \leq 1, \quad \left|E_N^{(2)}(\lambda,\phi)\right| \leq 1, \tag{6.21}$$

one can derive the following Bell inequality along the lines of Bell's original proof for $N = 1$:

$$S_N = |E_N(\theta,\phi) - E_N(\theta,\phi') + E_N(\theta',\phi) + E_N(\theta',\phi')| \leq 2. \tag{6.22}$$

For realizable situations to date involving photodetectors, the probability of detecting a total of $N$ photons at $C$ and $D$ is small even where one has precisely $N$ photons incident on each analyzer, because of the detection inefficiencies. Thus $E_N(\theta,\phi)$ is small and the inequality not violated. One may introduce an auxiliary assumption to allow a testable experiment by considering only measurements over the subensemble where a total of $N$ photons are detected at both $C$ and $D$. One defines

$$S_N^{(1)}(\lambda,\theta) = \frac{P_N^{(1)}(\lambda,\theta) - P_{N-1}^{(1)}(\lambda,\theta) + P_{N-2}^{(1)}(\lambda,\theta) - \cdots}{P_N^{(1)}(\lambda,\theta) + P_{N-1}^{(1)}(\lambda,\theta) + P_{N-2}^{(1)}(\lambda,\theta) + \cdots} \tag{6.23}$$

and similarly

$$S_N^{(2)}(\lambda,\theta) = \frac{P_N^{(2)}(\lambda,\theta) - P_{N-1}^{(2)}(\lambda,\theta) + P_{N-2}^{(2)}(\lambda,\theta) - \cdots}{P_N^{(2)}(\lambda,\theta) + P_{N-1}^{(2)}(\lambda,\theta) + P_{N-2}^{(2)}(\lambda,\theta) + \cdots}. \tag{6.24}$$

Rearranging one obtains

$$E_N(\theta,\phi) = \int f(\lambda) S_N^{(1)}(\lambda,\theta) S_N^{(2)}(\lambda,\phi) d\lambda, \tag{6.25}$$

where

$$f(\lambda) = \rho(\lambda)\left\{P_N^{(1)}(\lambda,\theta) + P_{N-1}^{(2)}(\lambda,\theta) + \cdots\right\} \times \left\{P_N^{(2)}(\lambda,\phi) + P_{N-1}^{(2)}(\lambda,\phi) + \cdots\right\} \tag{6.26}$$

is the probability distribution for the subensemble. With the assumption $\left|S_N^{(1)}(\lambda,\theta)\right| \leq 1$ and $\left|S_N^{(2)}(\lambda,\phi)\right| \leq 1$, and assuming $f(\lambda)$ is independent of $\theta$ and $\phi$ (this is the auxiliary assumption), one can derive the normalized inequality

$$\bar{S}_N = \left|\bar{E}_N(\theta,\phi) - \bar{E}_N(\theta,\phi') + \bar{E}_N(\theta',\phi) + \bar{E}_N(\theta',\phi')\right| \leq 2, \tag{6.27}$$

where $\bar{E}_N(\theta,\phi)$ is the product $E_N(\theta,\phi)$ calculated over

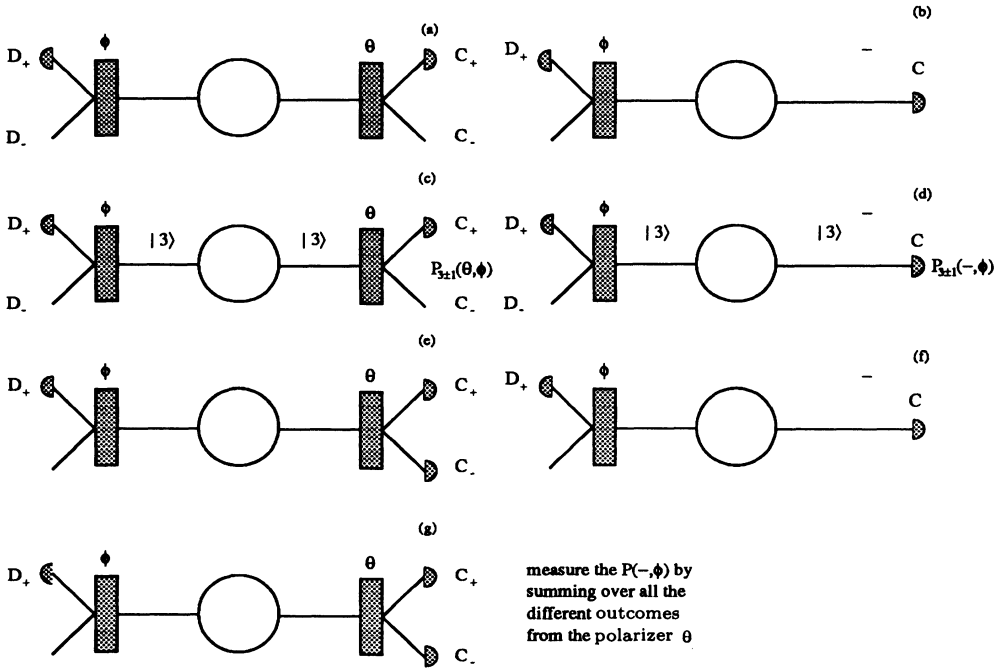


FIG. 22. Possible experimental configurations for a test of the CHSH inequality for (a) a measurement of the joint probability $P_N(\theta,\phi)$ with two detectors and two analyzers, (b) a measurement of the joint probability $P_N(-,\phi)$ with two detectors and one analyzer, (c) a measurement of the joint probability $P_{3\pm1}(\theta,\phi)$ with two detectors and two analyzers for the case of a $|3\rangle|3\rangle$ photon-number state input [the outcomes where three photons and two photons are detected at each detector will both contribute to the experimenter's calculation of $P_{3\pm1}(\theta,\phi)$], (d) a measurement of the joint probability $P_{3\pm1}(-,\phi)$ with two detectors and one polarizer for the case of a $|3\rangle|3\rangle$ photon-number state input [the situations where three photons and two photons are detected at each detector will both contribute to the experimenter's calculation of $P_{3\pm1}(\theta,\phi)$], (e) a measurement of the joint probabilities with three detectors and two analyzers for the case of parametric down-conversion, (f) a measurement of the one-sided joint probabilities with two detectors and one polarizer for the case of the parametric down-conversion, and (g) a measurement of the one-sided joint probabilities with three detectors and two polarizers for the case of parametric down-conversion.

the reduced ensemble.

Previously the weaker inequality (6.27) has been used for situations where a precise number of photons is (assumed) incident on each analyzer at $C$ and $D$, but (because of poor detector efficiencies) the probability of all the photons being detected and hence contributing to the measured subensemble is actually small. Our use of the inequality in Secs. IV and V is somewhat broader. Let us select to measure the $N$th-order correlation $\bar{S}_N$ or $S_N$. For higher $r$ values, there is a significant probability that the source emits greater than $N$ photons into each signal and idler field. We are thus considering our measured subensemble to be one where not necessarily all of the photons are detected. The standard auxiliary assumption still applies here: that for every $\lambda$, the probability of detection of a total of $N$ photons at $C$ (and a total of $N$ photons at $D$) is independent of the analyzer angle $\theta$ (and $\phi$).

## VII. THE VALIDITY OF AUXILIARY ASSUMPTIONS IN THE CASE OF NOISY DETECTION

In the recent nondegenerate parametric down-conversion experiment of Smithey *et al.* [16], subshot noise photon-number correlations for twin pulses each with approximately $10^6$ photons were demonstrated. Here one was able to use photodiodes with $85-90\,\%$ quantum efficiency. Thus it is possible to work in a truly macroscopic regime with the high efficiencies indicated in Figs. 16 and 17. However, a new limitation does become apparent. Electronic noise limits the resolution available in determining $N$, the number of photons. In the experiment demonstrating subshot noise performed by Smithey *et al.* with $N = 10^6$ photons the uncertainty in this photon number was of order $\Delta N = 324$.

We need to examine the effect of this reduction in resolution of photon number detected on the Bell-inequality experiments we have proposed. Let us consider the $N$th-order Clauser-Horne experiment as seen in Fig. 22(a) for the $P_N(\theta,\phi)$ measurement and in Fig. 22(b) for the $P_N(-,\phi)$ case. In the Clauser-Horne inequality we have the auxiliary assumption that requires

$$P_N^{(1)}(\lambda,\theta) \le P_N^{(1)}(\lambda,-), \quad P_N^{(2)}(\lambda,\phi) \le P_N^{(2)}(\lambda,-). \tag{7.1}$$

If one requires the use of extra detectors at $C_-$ and $D_-$ as in the down-conversion experiments for higher $r$, one has the auxiliary assumption (6.18). This condition must be satisfied for the inequality to be valid. These assumptions are reasonable when dealing with inefficient detectors. What happens when we have poor resolution instead of inefficient detectors?

### A. An idealized situation using correlated photon-number states

Consider the case where we have $N$ photons incident at $C$ and $D$. Let us consider our poor resolution to mean that our detectors could detect $N\pm\Delta N$ photons. Here we use the notation $N\pm\Delta N$ to mean the subset of $N-\Delta N$, $N-\Delta N+1$, ..., $N+\Delta N-1$, $N+\Delta N$, which is zero or positive. We would measure the quantities $P_{N\pm\Delta N}(\theta,\phi)$ and $P_{N\pm\Delta N}(-,\phi)$. For the case $N=3$, $\Delta N=1$, we have [Figs. 22(c) and 22(d)] (here we do not add the additional detectors at $C_-, D_-$)

$$\begin{aligned} P_{3\pm1}(\theta,\phi) &= P_{3,3}(\theta,\phi) + P_{3,2}(\theta,\phi) \\ &\quad + P_{2,3}(\theta,\phi) + P_{2,2}(\theta,\phi), \\ P_{3\pm1}(-,\phi) &= P_{3,3}(-,\phi) + P_{3,2}(-,\phi) \\ &\quad + P_{2,3}(-,\phi) + P_{2,2}(-,\phi), \end{aligned} \tag{7.2}$$

where $P_{i,j}(\theta,\phi)$ is the probability of detecting (with perfect resolution) $i$ photons at $C_+$ and $j$ photons at $D_+$. The $P_{i,j}(-,\phi)$ is similarly defined, but with no analyzer at $C$. According to a local hidden variable theory, we can write the generalizations of (6.12)–(6.14). Thus, for example,

$$P_{N\pm\Delta N}^{(12)}(\theta,\phi) = \int \rho(\lambda) P_{N\pm\Delta N}^{(1)}(\lambda,\theta) P_{N\pm\Delta N}^{(2)}(\lambda,\phi)\, d\lambda, \tag{7.3}$$

$$P_{N\pm\Delta N}^{(12)}(-,\phi) = \int \rho(\lambda) P_{N\pm\Delta N}^{(1)}(\lambda) P_{N\pm\Delta N}^{(2)}(\lambda,\phi)\, d\lambda, \tag{7.4}$$

and the auxiliary assumption (6.16) becomes

$$0 \le P_{N\pm\Delta N}^{(1)}(\lambda,\theta) \le P_{N\pm\Delta N}^{(1)}(\lambda), \tag{7.5}$$

$$0 \le P_{N\pm\Delta N}^{(2)}(\lambda,\theta) \le P_{N\pm\Delta N}^{(2)}(\lambda). \tag{7.6}$$

The assumption is that for every emission $\lambda$, the probability of detecting $N\pm\Delta N$ photons is never greater than that without a polarizer.

Importantly, however, because many situations of poor photon-number resolution will actually correspond to high $N$ situations where detector efficiencies may be high, it may not be necessary to use weaker inequalities. One could consider testing the stronger inequality in the poor resolution situation. Here one defines the marginal probabilities, for example, $P_{3\pm1}^{(2)}(\phi) = P_3^{(2)}(\phi) + P_2^{(2)}(\phi)$ and $P_{3\pm1}^{(1)}(\phi) = P_3^{(1)}(\phi) + P_2^{(1)}(\phi)$ as the extensions of the probabilities defined in (6.3)–(6.5). The stronger Clauser-Horne inequality can be derived:

$$B_{N\pm\Delta N} = \frac{P_{N\pm\Delta N}^{(12)}(\theta,\phi) - P_{N\pm\Delta N}^{(12)}(\theta,\phi') + P_{N\pm\Delta N}^{(12)}(\theta',\phi) + P_{N\pm\Delta N}^{(12)}(\theta',\phi')}{P_{N\pm\Delta N}^{(1)}(\theta') + P_{N\pm\Delta N}^{(2)}(\phi)} \le 1. \tag{7.7}$$

### B. The parametric amplifier

One can calculate the effect of noisy resolution in the case of correlated photon-number states. However, in the parametric amplifier case the system is a summation of many correlated photon-number states, as given by Eq. (4.2). In this case we use (for both Clauser-Horne and product inequalities) an extra detector in an attempt to prepare the appropriate subensemble by ensuring that the sum of the photons at both $C_+, C_-$ and $D_+, D_-$ is equal to $N$. Because of the limited resolution, the state preparation will not be precise. Such an experiment is depicted in Fig. 22(e). Now for this arrangement, one still requires use of an auxiliary assumption, even though one may have perfect detectors, because we are restricting measurements to a particular subensemble. The question that must be asked is whether the auxiliary assumptions of the type (6.18) are reasonable. The assumptions will break down. Let us examine again the case of $N = 3$, $\Delta N = 1$. The possible states contributing to the measurement are $|2\rangle, |3\rangle, |4\rangle, |5\rangle$, which can be seen from the following analysis of which detections will be interpreted by the experimenter within the limits of his resolution as contributing to the relevant subensemble:

$$\begin{aligned} &C_+ \text{ detects } 3 \pm 1 \text{ while } C_- \text{ detects } 0 \pm 1 \text{ photons,} \\ &C_+ \text{ detects } 2 \pm 1 \text{ while } C_- \text{ detects } 1 \pm 1 \text{ photons,} \\ &C_+ \text{ detects } 1 \pm 1 \text{ while } C_- \text{ detects } 2 \pm 1 \text{ photons,} \\ &C_+ \text{ detects } 0 \pm 1 \text{ while } C_- \text{ detects } 3 \pm 1 \text{ photons;} \end{aligned} \tag{7.8}$$

$$C_+ \text{ and } C_- \text{ together can detect } 2,\ 3,\ 4,\ \text{or } 5 \text{ photons.} \tag{7.9}$$

For example, the outcome which the experimenter records as 3 photons at $C_+$ and 0 photons at $C_-$ may arise from detection of $3 \pm 1$ and $0 \pm 1$ photons at $C_+$ and $C_-$, respectively. First we notice from the case, for example, where we actually detect 3 photons at $C_+$ and 2 photons at $C_-$ that the state $|5\rangle$ does contribute to the required subensemble. However, the outcome where we detect 5 photons at $C_+$ and 0 photons at $C_-$ is not included by the experimenter as contributing. Hence we can see that the probability distribution for detection may depend on $\theta, \phi$ and hence the auxiliary assumption used in the derivation of the usual Bell inequality (6.27) is not valid. The total number of counts for a particular $\theta$ and $\phi$ is not independent of $\theta$ and $\phi$.

The addition of the extra detector in the Clauser-Horne-type experiment also causes a breakdown of the auxiliary assumptions (7.5) and (7.6). Let us consider now the experiment used to determine $P_{N\pm\Delta N}(-,\phi)$ [shown in Fig. 22(f)]. It can be seen that on the side with no polarizer (and hence only one detector) the state $|5\rangle$ does not contribute at all, whereas it will contribute to the measurement of $P_{N\pm\Delta N}(\theta,\phi)$. Thus the auxiliary assumption is not valid. We might consider modifying the scheme to include two detectors for this "no-polarizer" measurement [Fig. 22(g)]. We would leave the second $\theta$ polarizer in and measure with two photon detectors both channels of the output from the polarizer. Now the probability $P_N(-,\phi)$ would be interpreted as the joint probability of detecting $N$ photons at $D_+$ and a total of $N$ photons at the $C_+$ and $C_-$ detectors. The auxiliary assumptions here would be that of the product case discussed above in Sec. VI B. This scheme, too, has problems. At the $C$ polarizer we have the outcomes (7.8) and (7.9) as considered relevant by the experimenter for the $N = 3$, $\Delta N = 1$, case. Now the experimenter would want to measure $P_{3,0,3}$ (3 photons at $C_+$, 0 photons at $C_-$, and 3 photons at $D_+$) say, but because of the poor resolution ($\Delta N = 1$), one would actually be monitoring the outcomes $3 \pm 1$ photons at $C_+$, $0 \pm 1$ photons at $C_-$, and $3 \pm 1$ photons at $D_+$. The experimenter then counts the number of times (measures the rate of such outcomes) the reading $(3,0,3)$ appears, but this is really the number of times one detects $(3,0,3)$, $(2,1,3)$, $(3,0,2)$, and $(3,1,2)$ at the output since the experimenter cannot distinguish between these. To determine the probability $P_{3 \text{ at } C_+,\ 0 \text{ at } C_-,\ 3 \text{ at } D_+}(\theta,\phi)$ we could have perfect event-ready detectors which tell us when there is an emission. Then the probability is

$$P_{3 \text{ at } C_+,\ 0 \text{ at } C_-,\ 3 \text{ at } D_+}(\theta,\phi) = \frac{[\text{number of times the reading } (3,0,3) \text{ occurs}]}{(\text{number of emissions})}. \tag{7.10}$$

Next one will wish to measure the result $P_{2 \text{ at } C_+,\ 1 \text{ at } C_-,\ 3 \text{ at } D_+}(\theta,\phi)$. If we examine the probabilities calculated we observe that detecting two photons at $C_+$ and one photon at $C_-$ contributes to both the (3,0,−) result and the (2,1,−) result. Hence it will be calculated twice and so our calculated "probabilities" would add to greater than one. Alternatively one could "normalize" by calculating the probabilities as follows:

$$P_{i,j,k} = \frac{P_{i,j,k}}{\sum_{i,j,k} P_{i,j,k}}. \tag{7.11}$$

Here, however, the sum of all probabilities $\sum_{i,j,k} P_{i,j,k}$ will contain terms such as (2,1,3) twice and hence will be dependent on the analyzer angles $\theta$ and $\phi$. This prevents the derivation of the usual "weaker" Bell inequalities. Thus one must be careful when determining a measurement scheme for the $P_{i,j,k}$. Note that experiments designed to test the product Bell inequality proposed here require the same care with auxiliary assumptions since these also, in the case of the parametric amplifier, require more than one detector at $C$ and the measurement of more than one $P_{i,j,k}$.

To conclude, testing the proposed $N$th-order Bell in-

equalities with a poor resolution of photon number detected can pose problems in the case where the incident state is generated by parametric amplification. This is because here states of $n$, where $n$ is not necessarily equal to $N$, photon number can be incident on the analyzers and cause a failing of the usual auxiliary assumptions which are introduced in this case (even where there is a high detection efficiency) to restrict measurements to the case $n = N$. These problems may be overcome where one has incident on the analyzers a state of precise photon number, so that the state preparation is done before passage through analyzers rather than after.

## VIII. CONCLUSION

We have shown how multiparticle and potentially macroscopic states predicted to violate a Bell inequality may be generated from the correlated photon-number states $\sum_{m=0}^{N} |m\rangle|N-m\rangle|m\rangle|N-m\rangle$ (the four-mode system) or $|N\rangle|N\rangle$ (the two-mode system). The proposed experiment is also a test of quantum mechanics for states of higher spin. The proposed experiments are extensions of those using parametric down-conversion to test quantum mechanics where one photon is incident on each analyzer. The inequality is tested by measurement of joint probabilities where $n$ photons are detected at one space-time point. The violation is evident for $n = N$ photons, but reduces dramatically for $n < N$, where one loses information about the $n - N$ photons.

The correlated photon-number states may be generated via parametric down-conversion. For poor detector efficiencies the sensitivity of the violation to the value of $n$ means that at larger gains the direct output of the parametric amplifier gives no violation. This is because the probability of the amplifier generating $|n+i\rangle|n+i\rangle$ (where $i > 0$), rather than $|n\rangle|n\rangle$, is significant. Hence violations are predicted only for regimes where the probability of actually generating the $|n\rangle|n\rangle$ state where $n$ is large is very small. Nevertheless consideration of experiments with $N = 2$ would not seem unreasonable. For higher detector efficiencies, it is possible to "prepare" the $|n\rangle|n\rangle$ state by restricting attention to the subensembles where only $n$ photons are detected at each of the spatially separated locations. Here auxiliary assumptions of the usual type are required. In this case, violations are obtained for all values of parametric gain. Unfortunately, the probability of actually detecting the appropriate $|n\rangle|n\rangle$ state is small because of the super-Poissonian photon-number distribution of the output signal and idler beams. Here we have limited consideration to a classically pumped parametric down-conversion.

Finally, we have included a discussion and preliminary calculation for the situation corresponding to the Smithey *et al.* experiment. Prior to this experiment, it seemed that the preparation using parametric down-conversion of the type of correlated photon states we consider would have been difficult for more than two or three photons in each beam. Yet in their recent experiment, Smithey *et al.* have demonstrated subshot noise photon-number correlations for twin pulses each with $10^6$ photons. Here one was able to use photodiodes with 85–90 % quantum efficiency. In terms of Bell's inequality a new limitation is electronic noise, which limits the resolution available in determining $n$, the number of photoelectrons. Unfortunately in the case of parametric down-conversion, with the form of "state preparation" we suggest here, the auxiliary assumptions used in the formulation of the classical inequality break down. However, if we could prepare a correlated photon-number system with only a small number of significant states, then a strong classical Bell inequality formulated without using auxiliary assumptions may be violated and hence there is the potential for a possible test of quantum mechanics in the truly macroscopic regime.


[1] J.S. Bell, Physics (N.Y.) **1**, 195 (1965); J.S. Bell, in *Foundations of Quantum Mechanics*, edited by B. d'Espagrat (Academic, New York, 1971), p. 171.

[2] J.F. Clauser and A. Shimony, Rep. Prog. Phys. **41**, 1881 (1978).

[3] A. Einstein, B. Podolsky, and N. Rosen, Phys. Rev. **47**, 777 (1935).

[4] A. Aspect, P. Grangier, and G. Roger, Phys. Rev. Lett. **49**, 91 (1982); A. Aspect, J. Dalibard, and G. Roger, *ibid.* **49**, 1804 (1982).

[5] D.C. Burnham and D.L. Weinberg, Phys. Rev. Lett. **25**, 84 (1970); S. Friberg, C.K. Hong, and L. Mandel, *ibid.* **54**, 2011 (1985); R. Ghosh and L. Mandel, *ibid.* **59**, 1903 (1987).

[6] Y.H. Shih and C.O. Alley, Phys. Rev. Lett. **61**, 2921 (1988); C.O. Alley and Y.H. Shih, in *Proceedings of the Second International Symposium on Foundations of Quantum Mechanics in the Light of New Technology*, edited by M. Namaki *et al.* (Phys. Soc. Jpn., Tokyo, 1986), p. 47.

[7] Z.Y. Ou and L. Mandel, Phys. Rev. Lett. **61**, 50 (1988).

[8] J.G. Rarity and P.R. Tapster, Phys. Rev. Lett. **65**, 2495 (1990).

[9] Z.Y. Ou, X.Y. Zou, L.J. Wong, and L. Mandel, Phys. Rev. Lett. **65**, 321 (1990); J.G. Rarity, P.R. Tapster, E. Jakeman, T. Larchuk, R.A. Campos, M.C. Teich, and B.E.A. Saleh, *ibid.* **65**, 1348 (1990); P.G. Kwiat, W.A. Vareka, C.K. Hong, H. Nathel, and R.Y. Chiao, Phys. Rev. A **41**, 2910 (1990); J. Brendel, E. Mohler, and W. Martienssen, Europhys. Lett. **20**, 575 (1992); P.G. Kwait, A.M. Steinberg, and R.G. Chiao, Phys. Rev. A **47**, 2472 (1993).

[10] P.D. Drummond, Phys. Rev. Lett. **50**, 1407 (1983).

[11] W.J. Munro and M.D. Reid, Phys. Rev. A **47**, 4412 (1993).

[12] W.J. Munro and M.D. Reid, Quantum Opt. **6**, 1 (1994).

[13] N.D. Mermin, Phys. Rev. D **22**, 356 (1980).

[14] S.L. Braunstein and C.M. Caves, Phys. Rev. Lett. **61**, 662 (1988).

[15] B.J. Oliver and C.R. Stroud, J. Opt. Soc. Am. B **4**, 1426

(1987).
[16] D.T. Smithey, M. Beck, M. Belsley, and M.G. Raymer, Phys. Rev. Lett. **69**, 2650 (1992).
[17] J.F. Clauser and M. Horne, Phys. Rev. D **10**, 526 (1974); J.F. Clauser, M.A. Horne, A. Shimony, and R.A. Holt, Phys. Rev. Lett. **23**, 880 (1969).
[18] D.M. Greenberger, M.A. Horne, and A. Zeilinger, in *Bell's Theorem, Quantum Theory and Conceptions of the Universe*, edited by M. Kafatos (Kluwer Academic, Dordrecht, 1989), p. 173; D.M. Greenberger, M.A. Horne, A. Shimony, and A. Zeilinger, Am. J. Phys. **58**, 1131 (1990); N.D. Mermin, Am. J. Phys. **58**, 731 (1990).
[19] N.D. Mermin, Phys. Rev. Lett. **65**, 1838 (1990).
[20] M.D. Reid and W.J. Munro, Phys. Rev. Lett. **69**, 997 (1992).
[21] M.D. Reid and D.F. Walls, Phys. Rev. A **34**, 1260 (1985).
[22] M.A. Horne, A. Shimony, and A. Zeilinger, Phys. Rev. Lett. **62**, 2209 (1989); M.A. Horne and A. Zeilinger, in *Proceedings of the Symposium on Foundations of Modern Physics*, edited P. Lahti and P. Mittelstaedt (World Scientific, Singapore, 1985).
[23] A.J. Leggett, in *Directions in Condensed Matter Physics*, edited by G. Grinstein and G. Mazenko (World Scientific, Singapore, 1986); S. Song, B. Yurke, and C.M. Caves, Phys. Rev. A **41**, 5261 (1990).
[24] M.D. Reid and D.F. Walls, Phys. Rev. Lett. **53**, 955 (1984).
[25] J.D. Franson, Phys. Rev. Lett. **62**, 2205 (1989); P. Grangier, M.J. Potasek, and B. Yurke, Phys. Rev. A **38**, 3131 (1988); S. Tan, D.F. Walls, and M.J. Collett, Phys. Rev. Lett. **66**, 252 (1991).
[26] P.L. Kelley and W.H. Kleiner, Phys. Rev. A **136**, 316 (1964).
[27] R. Graham, Phys. Lett. **32A**, 373 (1970); Phys. Rev. Lett. **52**, 117 (1984).
[28] M.J. Collett and D.F. Walls, Phys. Rev. A **32**, 2887 (1985); M.J. Collett and C.W. Gardiner, *ibid.* **30**, 1386 (1984); C.W. Gardiner and M.J. Collett, *ibid.* **31**, 3761 (1985).
[29] P.D. Drummond and C.W. Gardiner, J. Phys. A **13**, 2353 (1980).
[30] K.J. McNeil and C.W. Gardiner, Phys. Rev. A **28**, 1560 (1983).